Chemical Reactor Models of Digestion Modulation

William Wolesensky* & J. David Logan
Department of Mathematics
University of Nebraska–Lincoln
Lincoln, NE 68588-0130

August 17, 2004

Abstract

In this paper we give an overview of the application of chemical reactor theory to models of digestion processes and indicate how those models extend to eco-physiological questions of modulation of digestion and feeding. In particular, we discuss processes that organisms may use to manage their nutrient intake, including optimality, ecological stoichiometry, and regulatory physiology. In the context of regulatory physiology we present a new, detailed model that forges an eco-physiological connection between animal foraging and digestion modulation. The discussion focuses on insect herbivores, in particular common grasshoppers and locusts. In presenting the highlights of reactor models we set up a mathematical model of pre- and post-ingestive changes that an insect may employ when faced with suboptimal foods. To achieve this post-ingestive change we employ a simple control mechanism that is dependent on the ratio of the concentration of two nutrients in the hemolymph. The control serves to limit the absorption of the nutrient that is occurring in excess, thus allowing the insect to avoid "jamming" the regulatory mechanisms that affect feeding. At the same time, pre-ingestive controls influence the inter-meal time period to allow insects to eat more frequently when feeding on suboptimal food. We examine the effect that the control mechanisms have on nutrient uptake by simulating feeding on two foods of different quality. Numerical simulations give results that are qualitatively congruent with empirical data.

1 INTRODUCTION

Chemical reactor models of the digestive system and its components have provided an important framework to quantitatively study physiological processes involved in food processing. One fundamental issue in eco-physiology is to link digestion to ecological factors, such as resource acquisition. For many years these two fields developed nearly independently. But there is now an increasing effort to show that pre-consumption and post-consumption events are intimately related and form a integrated picture of the overall, whole individual. In this paper we show how the chemical reactor paradigm is useful in developing this link by including feedbacks and controls that dictate foraging behavior. The specific goal of the paper is

*Permanent address: Program in Mathematics, College of Saint Mary, Omaha, NE 68124.

twofold: first, to give an overview of modeling digestion processes by chemical reactor theory, and show how digestion modulation can occur through optimization, or through maintaining homeostasis in a context of regulatory physiology or ecological stoichiometry; and second, to present a new, detailed model of digestion modulation in the context of regulatory physiology that provides a connection between foraging and digestion. Although the discussion is focused on insect herbivores, and, in particular, common grasshoppers and locusts, it may be applicable to other taxa.

It is not hard to imagine that the digestive structure of an insect herbivore is much like an industrial chemical processing plant. Chemical reactants (nutrients, elements) are fed into the system, reactions occur, and the products are used to supply the energy to drive the reactor itself and carry out all of the activities required, including growth, reproduction, maintenance, as well as provide the energy to find resources in the first place. Although chemical reactor theory, in the context of chemical engineering, had been used for decades to design industrial applications, it wasn't until the mid 1980s that D. L. Penry and P. A. Jumars applied the ideas to digestion processes in simple organisms. Now, this chemical reactor modeling strategy has been applied to numerous animal gut designs, and it has provided a quantitative framework for addressing many complex questions about digestion processes in both vertebrates and invertebrates up and down the complexity scale. Furthermore, many experimental studies have shown that food acquisition and food processing are not independent processes. That this should be true is intuitively clear. It has been confirmed by many experiments that an animal's environment, habitat, and diet can affect gut morphology and food processing rates, while physiological cues and processes can trigger hunger and subsequent foraging activities.

Chemical reactor models provide a framework for linking physiological activities to ecological ones. For example, a foraging response (a gustatory response) can be stimulated by chemical signals in the metabolic pathways of the organism. One way this can occur is through nutrient concentrations in the circulatory system. When a certain nutrient or chemical concentration falls below some threshold level, a gustatory response results. When the concentration exceeds some upper target threshold, feeding ceases. Also, other cues, like defecation and stresses in the gut itself, can induce feeding or the the cessation of feeding. Chemical reactor theory, by design, enables one to calculate concentrations in the reactor, input and output rates, chemical kinetics, absorption rates, and so on. All of these can provide feedbacks and controls on organism activities. By linking different types of reactors one can monitor concentrations in different portions of the digestive system, e.g. in both the midgut and hemolymph of an insect.

In the first part of this paper we review some of the important developments in chemical reactor applications to digestion in simple organisms. We define the different types of reactors and discuss their role in modeling different types of gut structures. The emphasis is on the quantitative features. We show how reactor theory can address questions of optimal strategies for food processing. Next we discuss how homeostasis can be a basis for regulation. This latter theory is developed in the contexts of ecological stoichiometry and regulatory physiology.

In the second part of the paper (Section 5) we analyze a specific organism and address the issue of how nutrient titers can influence gustatory responses and subsequent foraging. The model is strongly motivated by the extensive and important experimental work of S. Simpson and D. Raubenheimer (references are given below) on gustatory responses in locusts. This model, set in the context of regulatory physiology, is resolved by numerical simulations, and we are able to calculate feeding responses when the animal is fed foods of different quality.

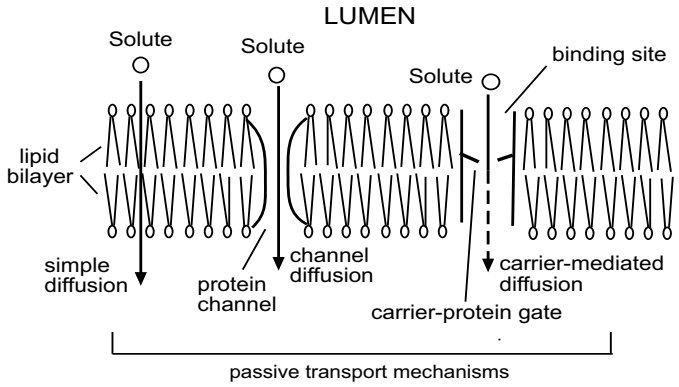

Figure 1: Schematic showing the lipid bilayer membrane and various solute transport mechanisms that permit nutrients in the lumen to cross the gut wall.

2 NUTRIENT ACQUISITION MODULATION

Viewed as a model process, nutrient acquisition can be idealized and simplified to the following serial steps: foraging, consumption of large macromolecules, breakdown into smaller units, absorption, and use of the newly acquired nutrients in the organism's energy budget. Fundamental questions in eco-physiology are: what modulates this process and how are different parts of the process interrelated?

The first step, foraging, is an extensive subject area and can be subdivided into search strategies, attack strategies, and food handling strategies. These are discussed in detail in Stephens & Krebs (1986). Digestion begins when the food is consumed. Carbohydrates, fats, and protein are broken down in parts of the gut into simpler compounds like sugars, alcohols and fatty acids, and amino acids. These can then be absorbed (or assimilated) across the gut wall into the animal's circulatory system where they are distributed to the organism's energy budget to carry out basic organism activities: maintenance and respiration, reproduction, growth or production, and storage. A portion allocated to maintenance drives the energy needs of the organism to search, attack, and handle food back at the first step of the acquisition process.

Nutrient absorption in invertebrates, with all their diverse strategies, is discussed in detail in Wright & Ahearn (1997). The epithelial surfaces of the gut represent a limiting barrier in the overall nutrient acquisition process. Absorption of the simple compounds, which are products of substrate breakdown, across these barriers can be accomplished through carrier-mediated transport or simple diffusion. The lipid bilayer, which forms the common structure of membranes, consists of two opposing phospholipid molecules with a polar hydrophilic group forming the head and a nonpolar hydrophobic tail composed of fatty acids. See figure 1. The membrane is impermeable to most water soluble molecules. Interspersed in the layer are integral protein molecules that mediate the transport of molecules across the membrane. They carry out the functions of the membrane and come in many types, depending upon their function. Sugars and amino acids are hydrophilic and will not cross membranes by passive diffusion, so the selective proteins catalyze the transmembrane movement of these hydrophilic substances. Because membranes are lipids, lipophilic molecules can cross easily by simple diffusion through the membrane.

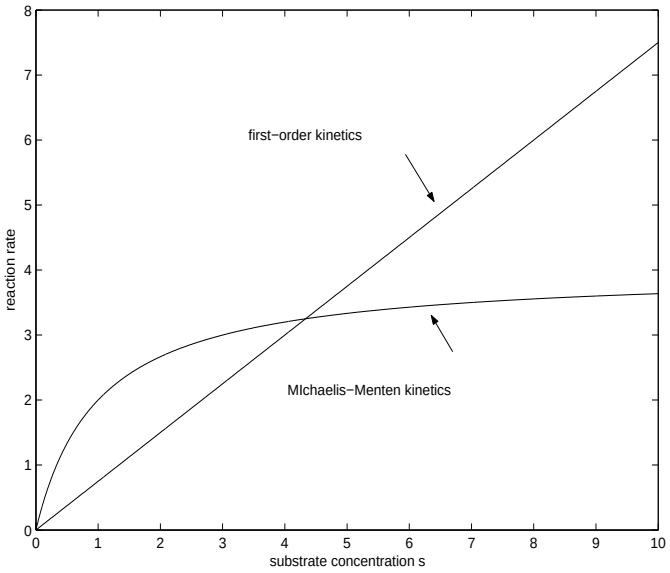

Figure 2: First-order and Michaelis-Menten kinetics.

The membrane transport proteins are of two types: carrier proteins that bind to solutes and act as gates through the membrane as reactions occur, and channel proteins that form hydrophilic pores that offer faster transport. Both of these types of transport, as well as simple diffusion, are passive transport mechanisms. Active transport mechanisms are protein binding sites that require energy (e.g., ATP) for transport of solutes.

From a mathematical modeling viewpoint, this electrochemical boundary through which fluxes occur is highly complicated. The usual approach is to model the detailed chemistry by simple reactions. First, we can model the breakdown of substrate molecules by enzyme reaction of the form $\mathbf{S} + \mathbf{E} \rightarrow \mathbf{E}+$ products, where $\mathbf{S}$ is a substrate (of concentration s) and $\mathbf{E}$ is an enzyme. These enzyme-substrate reactions are assumed to have reaction rate

$$R = \frac{k_m s}{k_h + s},$$

where k_m is the maximum rate (saturation) and k_h is the concentration at half-saturation. This is the usual Michaelis-Menten form. For simpler reactions, for example, $\mathbf{S} \rightarrow$products, we assume first-order kinetics,

$$R = ks,$$

where k is the rate constant. These forms are plotted in figure 2. For membrane transport, or absorption, we use first-order kinetics for simple diffusion or channel diffusion, and Michaelis-Menten kinetics for carrier-mediated transport. See Alberts (1994) for a full discussion of membrane transport. Many books discuss Michaelis-Menten kinetics; Edelstein-Keshet (1988) and Murray (2002), for example, give simple mathematical derivations of the Michaelis-Menten law based upon singular perturbation methods and chemical kinetics theory.

Some digestive physiologists rightfully feel uncomfortable with "assuming away" the detailed chemical kinetics as is often done in developing mathematical models.

But this strategy has been successful in inventing qualitative models that capture some of the important features of real processes. Models sacrifice precision and realism to provide qualitative information about the whole organism. In all models there is a hierarchy that involves making judgments of selecting variables, determining what interactions to include, identifying limiting steps, all with the desirability of omitting complications. Model problems in many areas have served to illustrate the broad interactions of different mechanisms and how those mechanisms affect important outcomes.

We also note the importance of temperature effects, especially in insects. Nutrient intake rates, substrate-breakdown rates, and absorption rates are all temperature dependent, and they strongly affect development rates, phenology, and feeding. To model temperature effects on digestion we can make the rate constants in the kinetics of both substrate-breakdown and absorption functions of body temperature. Because body temperature is imposed from environmental temperature, we do not need separate energetics for temperature variation. Typically, we use the Q_{10}-rule (defined below) to determine the magnitude of the temperature effects upon the reaction rates in our model of digestion modulation in Section 5.

Once nutrients cross the gut boundary they are distributed to the metabolic pathways and provide for the energy needs of the organism. The circulatory system (or the hemolymph in an insect) can be regarded as a chemical reactor, a pool for nutrients that are then allocated to the energy budget. Looked at in this way, nutrients are "currency" that an organism distributes to meet its needs. A certain amount is drained for basal maintenance and respiration, and then the rest is used for structure (growth and production) and reproduction. Excess amounts may be stored to meet later needs. It is also in this pool where threshold nutrient levels can trigger and control gustatory responses, or feedbacks that characterize the physiological-ecological link. Introductions to the concepts of energy budgets, as applied in our models, can be found in Gurney & Nisbet (1998), Lika & Nisbet (2000), or Kooijman (2000).

Now that we have reviewed the basic ideas in nutrient acquisition, we can ask what drives it. What modulates portions of this multi-step process and how do those components interrelate?

Karasov & Hume (1997) present in their review an excellent rationale for optimality. The key issue in optimization arguments is to select the objective function, i.e., the function to be maximized or minimized. Going back to a fundamental paper by Sibly (1980), one can reason that an organism performs so that it maximizes the rate that energy is obtained. Quantitatively, these arguments can be presented and analyzed in the context of the chemical reactor paradigm, as discussed below. For example, modulation occurs when an organism selects an optimal food retention time by maximizing its average net intake over that time. These relationships were first examined by Penry & Jumars (1986, 1987) for a variety of gut designs, and later authors applied the theory to specific taxa. Selection of this objective function, however, proved to be incorrect for certain species, and alternatives have been proposed. For example, time minimization has been one criterion–get the food through the system as fast as possible with extraction efficiency.

Another possible consumer strategy, which we follow in our discussion below, is to reach a nutritional goal, or target, by regulating nutrient intake. This tactic has been called "satisficing". This can be accomplished in different ways: through food selection, regulating assimilation across the gut wall, or selective excretion of certain over abundant or excess nutrients. Closely related is a strategy of homeostasis maintenance, which we review below. For homeostasis an organism maintains

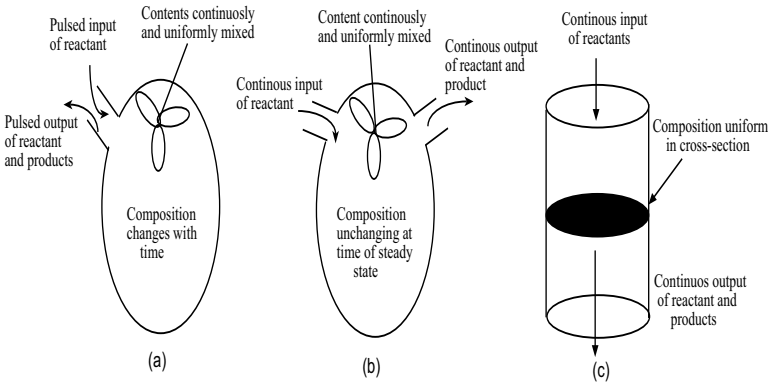

Figure 3: Three types of chemical reactors: (a) batch reactor (BR), (b) continuously stirred tank reactor (CSTR), and (c) plug flow reactor (PFR).

tight control on nutrient ratios (e.g., its C:N ratio) in its system, either expelling excess nutrients through excretion or egestion, or limiting excess nutrients through differential assimilation.

Still other strategies have been posed. In optimal foraging (e.g., see Belovsky 1997), relations between allometric quantities, food characteristics, and digestion characteristics (food residence time) lead to a constrained optimization problem where time and capacity are limiting quantities. Other strategies involve regulation of temperature, water, and/or pH. Yet another strategy, especially when food is scarce or is changed, is to compensate by changing the morphology of the gut, although the time scale over which this can occur may be much longer than the time scale for food availability changes. See Whelan & Schmidt (2003) for a review of digestive strategies.

3 CHEMICAL REACTOR MODELS

A chemical reactor model, or chemostat model, is an idealization of a complex process. Biochemical reactions and the overall electrochemistry of digestion is complicated and not thoroughly documented or understood in all taxa. As is the case for all mathematical models, the chemical reactor provides a caricature of the real situation, stripped down to essential elements with many of the fine details ignored. The idea of a model is not to make exact quantitative predictions, but to indicate the important qualitative features of the biological processes. Basically, a chemical reactor is a spatial unit, or volume, where chemicals are fed in, react, and then finally are absorbed or ejected. The fundamental physical law that gives rise to the model equations is mass conservation: the rate of change of the mass of a constituent inside the volume must equal the rate that the constituent flows in, plus (minus) the rate it is formed (consumed) by chemical reaction, minus the rate it is absorbed, minus the rate it flows out. It is common to identify three types of reactors: a batch reactor (BR), a continuously stirred tank reactor (CSTR), and a plug flow reactor (PFR). These are shown in figure 3. BRs process food in discrete portions. In a BR the reactants are loaded instantaneously at time $t = 0$, when the clock starts. Then the reactions occur over a time T (the residence time), and at the end the reactor is instantaneously emptied. BRs are appropriate for model-

ing, for example, the gastro-vascular cavities in some invertebrates like hydra and coelenterates; the cavity is filled quickly, reaction and absorption occur, then the material is expelled quickly. CSTRs provide for continuous flow in and out of the reactor. CSTRs provide models of large sacular gut chambers, like a crop (foregut) or stomach. CSTRs can operate in a steady state, where the input rate equals the output rate and concentrations are constant, or it can operate in a time-dependent manner where concentrations and flow rates are variable. A CSTR that is loaded instantaneously at time $t = 0$ and then empties over time is called a semi-batch reactor. In both BRs and CSTRs there are no spatial concentration gradients of reactants or products, and the contents are uniformly and continuously mixed. This uniformity property is an idealization because we often think of absorption occurring only along the boundary of the reactor, i.e., along the gut lining, which would in fact induce concentration gradients from the boundary to the interior of the gut volume. PFRs, or tubular reactors, model tubular gut structures such as a midgut structure, a hindgut, or some kind of intestine. In a PFR reactants, say contained in a bolus, flow continuously into the inlet at one end and react as they pass through. In the radial direction it is assumed there are no concentration gradients (uniform mixing in the radial direction), but in the axial direction there is variation. Thus, in each cross-section the concentrations are assumed to be constant. Again this is an idealization for absorption or for conversion reactions that take place on the boundary.

Penry & Jumars (1986, 1987), Woods & Kingsolver (1999), and Jumars (2000a) have laid out basic equations for different types of gut structures. A qualitative discussion with additional references, especially for the digestive system in mammals, is given in Martínez del Rio *et al* (1994). Here we present an overview in a general case. Chemical reactor models can be found in textbooks on reaction kinetics (e.g., see Nauman 1987).

3.1 Batch Reactors (BRs)

To model a BR of volume V we let $n_j = n_j(t)$ be the concentration (mass per volume) of the jth ($j = 1, 2, ..., J$) chemical species $\mathbf{N}_j$ in the reactor at time t, with $n_j(0) = n_{j0}$ being the initial concentrations of the load. We will often refer to the $\mathbf{N}_j$ as *nutrients,* but they may be substrates, enzymes, elements, or products of substrate breakdown. Ecological stoichiometry deals with elements, whereas regulatory physiology deals with nutrients (protein, carbohydrates, fats); detailed physiology is concerned with the actual chemical species themselves and exact, resolved chemical reactions.

By mass balance, the rate of change of the mass of the jth constituent in the reactor is equal to rate R_j that it is created (positive) or consumed (negative), less the of rate W_j of absorption at the boundary. In symbols,

$$\frac{d}{dt}(Vn_j) = VR_j(n_1, ..., n_J) - VW_j(n_1, ..., n_J), \quad j = 1, 2, ..., J. \tag{1}$$

Both rates may depend upon concentrations of the constituents, and on temperature (which in not indicated in the notation), and they are given in mass per unit time per volume. Since V is constant, it may be cancelled from these equations. The reaction rates R_j are specified by the chemical kinetics of reaction, or the law of mass action, and the absorption rates W_j depend upon the type of transport across the gut boundary (simple diffusion or carrier mediated transport). Equations (1) form a J-dimensional dynamical system of differential equations in nutrient space

$(n_1, ..., n_J)$. In general they are nonlinear and cannot be solved in analytic form. The behavior of the solutions of (1) can be complex, including chaotic regimes.

Typically, to study optimality and modulation of digestion processes in BRs we are interested in the dynamics and the total amount of nutrient uptake over a given residence time, or holding time, T. For example, suppose a single nutrient $\mathbf{N}$ is created by the one-step reaction $\mathbf{A} \to \mathbf{N}$ with first order kinetics $R = -ka$, where k is the rate constant, and the absorption rate of the nutrient has the Michaelis-Menten form $W = \frac{k_m n}{k_h + n}$. Then the dynamics is

$$\frac{dn}{dt} = k(a_0 - n) - \frac{k_m n}{k_h + n}, \quad n(0) = 0,$$

where a_0 is the initial concentration of $\mathbf{A}$. The steady state, or equilibrium, concentration is found by setting $dn/dt = 0$. In the present case there is a single positive stable equilibrium at

$$\overline{n} = \frac{1}{2}\left[a_0 - k_h - \frac{k_m}{k} + \sqrt{(a_0 - k_h - \frac{k_m}{k})^2 + 4a_0 k_h}\right],$$

so the concentration n in the gut steadily increases from its zero initial value, approaching the equilibrium concentration $\overline{n}$.

One way to assess the efficiency of a BR is to determine the time T it takes to achieve a given conversion. Here we investigate a different question, namely, what is the optimum time to keep the food in the gut, considering there is a cost to obtaining the food and a cost to digest it.

We illustrate modulation through optimality using the example above. The issue is how long should an animal whose gut is modeled by a BR retain the contents before expulsion. There is a digestion cost in retention and a foraging cost for obtaining the food in the first place (including finding, capturing, and handling food, and avoiding predators). We can argue as follows, equating the nutrient to energy currency. The uptake across the gut wall over a residence time T is

$$U(T) = \int_0^T V \frac{k_m n(s)}{k_h + n(s)} ds.$$

The uptake $U(T)$ plots as an increasing sigmoid-shaped curve. If we assume the total cost is $C+DT$, where C is a constant foraging cost and DT is the digestion cost, proportional to time in the gut T, then the net uptake is $E(T) = U(T) - C - DT$, where we have subtracted the costs. The strategy is to maximize the average net uptake, or energy gain, over the residence time T, and choose the optimum residence time to be the time that maximizes $E(T)/T$. From calculus we see that

$$\frac{d}{dT}\left(\frac{E(T)}{T}\right) = \frac{T(U'(T) - D) - (U(T) - C - DT)}{T^2} = \frac{TU'(T) - U(T) - C}{T^2}.$$

Therefore the optimal residence time T_{opt} is the time for which the numerator is zero, or

$$U'(T_{\text{opt}}) = \frac{U(T_{\text{opt}}) - C}{T_{\text{opt}}}.$$

This result has an interesting interpretation in time-energy space (figure 4) that allows us to calculate T_{opt} graphically. It requires that the slope of the curve $U(T) - C$ at the optimum residence time is the same as the slope of the straight line connecting the origin to the point $(T_{\text{opt}}, U(T_{\text{opt}}) - C)$ on the curve. Generally, we expect

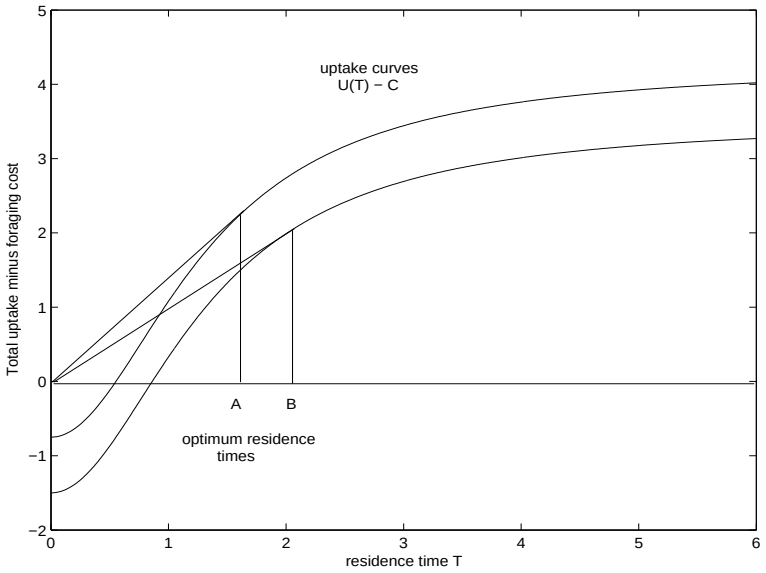

Figure 4: Two curves showing the total uptake minus the foraging cost for two different foraging costs. The optimal residence times A and B occur when the straight line emanating from the origin is tangent to the curves. These are the points of diminishing returns. Note that a larger foraging cost (lower curve) gives a longer residence time.

that the uptake curve $U(T)$ is a sigmoid shaped curve, so the optimal retention time may be found graphically. This is basically the marginal value theorem in economics where it is argued that a total resource, after an initial gain, begins in time to show diminishing returns; the intersection of the straight line from the origin and the net gain function is the point to "sell off" the resource. We also observe that if the foraging costs are higher, the uptake graph is shifted further downward and the tangent line criterion will give a longer residence time; so, the greater the cost of foraging, the longer the organism retains food. Sibly (1980) was the first to apply these ideas to digestion processes. See also Karasov (1988), and Martínez del Rio *et al* (1994). Clearly, chemical reactor models allow for a quantitative assessment of the basic concepts.

3.2 CSTRs

CSTRs, which model sacular organs, are more versatile in that they permit inflow (a feed) and outflow. If $q_{\text{in}}(t)$ and $q_{\text{out}}(t)$ represent time-dependent volumetric flow rates (volume per time) in and out of the reactor, then the volume of the lumen is time-dependent and given by $V(t) = V_0 + t(q_{\text{in}}(t) - q_{\text{out}}(t))$, where V_0 is the initial volume. If $n_j^{\text{in}}(t)$ denotes the concentration of the jth nutrient in the feed, then the mass balance law (1) is modified by adding the input and subtracting the output, or

$$\frac{d}{dt}(V(t)n_j) = q_{\text{in}}(t)n_j^{\text{in}}(t) - q_{\text{out}}(t)n_j + V(t)R_j(n_1, ..., n_J) - V(t)W_j(n_1, ..., n_J), \quad (2)$$

$j = 1, 2, ..., J$. This system of J differential equations for the nutrient concentrations cannot generally be resolved by analytic means, but must be solved numerically. Under certain assumptions, however, (2) may be reduced to a tractable problem. If the volumetric flow rates are the same (say, q) and the feed concentration is constant, then the system reduces to the autonomous system

$$\frac{dn_j}{dt} = \frac{q}{V}(n_j^{\text{in}} - n_j) + R_j(n_1, ..., n_J) - W_j(n_1, ..., n_J), \quad j = 1, 2, ..., J. \tag{3}$$

Most authors have studied CSTR digestion processes under the steady state assumption of constant nutrient concentrations, which satisfy the J algebraic conditions

$$\frac{q}{V}(n_j^{\text{in}} - n_j) + R_j(n_1, ..., n_J) = W_j(n_1, ..., n_J). \tag{4}$$

Jumars (2000a) considers the interesting, simple case of a substrate $\mathbf{N}_1$ entering the reactor and breaking down into a nutrient $\mathbf{N}_2$ that is then absorbed across the gut boundary. The reaction is $\mathbf{N}_1 \stackrel{k}{\rightarrow} \mathbf{N}_2 \stackrel{a}{\rightarrow}$ absorption, with $R_1 = -kn_1$ and $W_2 = an_2$. From (3) the governing equations are

$$\begin{aligned} \frac{dn_1}{dt} &= \frac{q}{V}(n_1^{\text{in}} - n_1) - kn_1, \\ \frac{dn_2}{dt} &= -\frac{q}{V}n_2 + kn_1 - an_2. \end{aligned}$$

In the steady state (equations (4)) we set the right sides equal to zero and solve for the equilibrium nutrient concentrations $n_1 = \overline{n}_1, \ \ n_2 = \overline{n}_2$. After performing some algebra we find that the equilibrium concentration of the nutrient is

$$\overline{n}_2 = \frac{qn_1^{\text{in}}kV}{(q + kV)(q + aV)}.$$

Therefore the total uptake rate J of the nutrient $\mathbf{N}_2$ is

$$J = aV\overline{n}_2 = \frac{qn_1^{\text{in}}akV^2}{(q + kV)(q + aV)}$$

We may now ask what flow rate q maximizes the uptake rate. Taking the derivative of J with respect to q and setting it equal to zero gives

$$q_{\text{opt}} = \sqrt{ak}V.$$

The maximum absorption rate is then

$$J_{\max} = \frac{n_1^{\text{in}}akV}{(\sqrt{k} + \sqrt{a})^2} = \frac{an_1^{\text{in}}V}{(1 + \sqrt{r})^2}, \quad r = \frac{a}{k}.$$

Observe that the volumetric flow rate (volume per time) is inversely proportional to the time the food is in the gut. We can gain important qualitative information from these formulas as follows. If $a \gg k$ ($r \gg 1$) the process is *digestion limited*; if $k \gg a$ ($1 \gg r$) the process is *absorption limited*. An organism suddenly faced with a lower quality of intake food n_1^{in} could compensate by increasing its gut size to maintain maximum efficiency; this corresponds to a larger q_{opt} and a shorter residence time. If food is low quality because it is difficult to extract, then k is small and the processes is again digestion limited and corresponds to a large r

value. The organism can again compensate by decreasing its residence time. Yang & Joern (1994) documented this behavior in grasshoppers–poor food quality is ejected quickly while high food quality is retained. Similar calculations may be made with Michaelis-Menten kinetics, although the algebra is more tedious.

Logan, Joern, & Wolesensky (2003) analyzed a time-dependent case where the gut is loaded instantaneously at $t = 0$ with a substrate and then emptied at a constant rate q, so that the volume is $V(t) = V_0 - qt$. This is the case of a semi-batch reactor that empties with residence time $T = V_0/q$. The reaction is $\mathbf{N}_1 \rightarrow \mathbf{N}_2 \rightarrow$ absorption, where $\mathbf{N}_1$ is the substrate and $\mathbf{N}_2$ is a nutrient product that is absorbed across the boundary. The reactor equations (2) become, for $t < T$,

$$\begin{aligned} \frac{d(V(t)n_1)}{dt} &= -qn_1 - V(t)R_1(n_1), \\ \frac{d(V(t)n_2)}{dt} &= -qn_2 - V(t)W_2(n_2), \end{aligned}$$

where R_1 is the substrate-product reaction rate and W_2 is the absorption rate of $\mathbf{N}_2$. Both rates could be either first-order or Michaelis-Menten. In this semi-batch case, when the derivative on the left sides of the equation is expanded, the flux terms cancel and we obtain the simple autonomous model

$$\begin{aligned} \frac{dn_1}{dt} &= -R_1(n_1), \\ \frac{dn_2}{dt} &= -W_2(n_2). \end{aligned}$$

The conditions $n_1(0) = s_0$ and $n_2(0) = 0$ give the initial substrate and product concentrations. If both rates are first order, i.e., $R_1 = kn_1$ and $W_2 = an_2$, then the system can be solved analytically.and the optimal residence time calculated as in the previous example. This time dependent model gives the same qualitative results as the CSTR operating in steady state, and it is discussed in detail in Logan, Joern, & Wolesensky (2003).

The model above can be extended to the case where the substrate input concentration n_1^{in} is a function of time t. Thus it measures a varying food quality. In this case the reactor equations are nonhomogeneous and have the form

$$\begin{aligned} \frac{dn_1}{dt} &= \frac{q}{V}(n_1^{\text{in}}(t) - n_1) - kn_1, \\ \frac{dn_2}{dt} &= -\frac{q}{V}n_2 + kn_1 - an_2. \end{aligned}$$

The initial conditions are $n_1(0) = n_2(0) = 0$, which means that concentrations of both the substrate and nutrient product are initially zero; for $t > 0$ substrate is input at the concentration $n_1^{\text{in}}(t)$, and the grazing rate q is assumed to be constant. This nonhomogeneous linear, two-dimensional system can be solved by standard methods (e.g., Ledder 2005) using the variation of parameters formula. The solution is

$$\begin{aligned} n_1(t) &= \frac{q}{V}\int_0^t n_1^{\text{in}}(\tau)e^{\lambda_1(t-\tau)}d\tau, \\ n_2(t) &= \frac{qk}{V(a-k)}\int_0^t n_1^{\text{in}}(\tau)\{e^{\lambda_1(t-\tau)} - e^{\lambda_2(t-\tau)}\}d\tau, \end{aligned}$$

where $\lambda_1 = -k - q/V$ and $\lambda_2 = -a - q/V$ are the eigenvalues of the of the matrix of the linear system. Therefore we can compute the rate of absorption of the nutrient

across the gut boundary as $VW_2 = Van_2$. Then the cumulative uptake of the nutrient over the length of a meal T is

$$U(T; n_1^{\text{in}}) = \frac{qak}{V(a-k)} \int_0^T \int_0^t n_1^{\text{in}}(\tau)\{e^{\lambda_1(t-\tau)} - e^{\lambda_2(t-\tau)}\}d\tau dt.$$

With a meal of given food quality, one can calculate the length of the meal T required to reach a target nutrient concentration C (i.e., *satisfice*) by numerically solving $U(T; n_1^{\text{in}}) = C$. We have mentioned this problem in the simple context of a CSTR in preparation for the discussion in Section 5 where absorption along the entire length of a tubular gut is modeled. There, the nutrients that are absorbed across the gut lining are distributed to an energy budget; target concentrations provide feed backs to initiate or shut down the feeding response.

Including a variable grazing rate $q = q(t)$ in the problem results in a nonhomogeneous linear system with variable coefficients. This makes the problem intractable with regard to analytic solution formulas. Moreover, for many organisms, e.g., locusts and grasshoppers, the grazing rate is often a function of food quality, and so depends on n_1^{in}. These issues are analyzed in Sections 5 and 6.

3.3 Tubular Reactors (PFRs)

In a tubular reaction chamber of length L and cross-sectional area A the concentrations of the nutrients $\mathbf{N}_j$ must be resolved in both space and time, so n_j is a function of two variables, $n_j = n_j(x,t)$, where x is the distance along the tubular gut from its inlet, $0 < x < L$. No variation is assumed in the radial direction, so concentrations in any cross-section are constant. The formulation of mass balance for tubular reactors leads to partial differential equations (reaction-advection equations) for the nutrient concentrations. A complete discussion and review is given in Logan, Joern, & Wolesensky (2002). See Edelstein-Keshet (1988) for a general discussion of reaction-advection processes. For a gut of constant cross-sectional area, the governing equations are,

$$\frac{\partial n_j}{\partial t} = -v\frac{\partial n_j}{\partial x} + R_j(n_1, ..., n_J) - W_j(n_1, ..., n_J), \tag{5}$$

$j = 1, 2, ..., J$, where v is the speed of the food bolus through the gut. Initial concentrations $u_j(x, 0)$ throughout the gut and concentrations $u_j(0, t)$ at the inlet must be specified to make the problem well-posed. But the concentrations at the exit point $x = L$ cannot be imposed; they are calculated as part of the solution. When the throughput speed is constant, this system of equations can be reduced to a system of ordinary differential equations by the transformation to a new coordinate z moving at the speed v of the bolus, i.e., $z = x - vt$. Under this transformation the advection term cancels and (5) becomes

$$\frac{\partial N_j}{\partial t} = R_j(N_1, ..., N_J) - W_j(N_1, ..., N_J), \quad j = 1, 2, ..., J,$$

where $N_j = N_j(z,t) = n_j(z + vt, t)$. Because no z-derivatives occur, this system is essentially a system of ordinary differential equations analogous to (3). This system is the one discussed by other authors (Penry & Jumars 1986, 1987; Jumars 2000a,b) when discussing PFR models of digestion operating in a steady state. We note that in many cases the reaction-advection system (5) can actually be solved analytically; these solutions are derived and catalogued in Logan, Joern,

& Wolesensky (2002) where temperature dependence, variable cross-sectional area, and location dependence is included.

In PFRs, the uptake across the boundary of the gut takes place along the entire gut length, perhaps at different rates depending upon the location. The total uptake $U_j(t)$ at time t of a nutrient $\mathbf{N}_j$ can be calculated by

$$U_j(t) = \int_0^L AW_j dx.$$

Using this expression we can discuss optimality issues of optimal retention time as in the case of BRs and CSTRs mentioned above.

Woods and Kingsolver (1999) account for radial variation in the absorption rate W_j in (5) by including a factor $2/r$, where r is the radius of the gut. If there is a fixed density of binding sites on the gut surface, then the number of sites in a length dx is proportion to $2\pi r dx$, and the number of molecules of the product molecules in the lumen is proportional to $\pi r^2 dx$. The ratio of transporters to molecules is $2/r$. As r increases there are proportionately fewer transporters in the wall per number of molecules in the corresponding lumen volume.

4 MODULATION THROUGH HOMEOSTASIS

Plants can vary widely in their nutrient content and thus their **C:N:P** ratios. In contrast, herbivore consumers are much less variable and stay within a restricted homeostatic range. This stoichiometric imbalance between herbivores and their food greatly affects consumer's growth, activity, and strategies to maintain homeostasis in its elemental ratios. There are two major views regarding how an organism modulates its intake and assimilation. One is based upon *regulatory physiology*, and the other is based upon *ecological stoichiometry*. In terms of regulatory physiology, organisms ingest proteins, fats, and carbohydrates, which are then broken down in highly regulated biochemical pathways during digestion; they are assimilated across the gut wall as nutrients, like amino acids, sugars, and phosphorus containing molecules. These nutrients cross the gut wall in definite proportions and are ultimately used in metabolism in smaller units to drive the organism's energy budget requirements. These molecules have repeatedly been shown to influence feeding and digestion (Brett 1993, Anderson & Hessen 1995, Tang & Dam 1999). Studies in insects have shown the importance of regulating protein and carbohydrate levels with corresponding consequences for individual performance (Simpson & Raubenheimer 1993b, 2000). For example, at the level of food intake, many organisms have sensory devices that regulate feeding based on these nutrients. Therefore, at the individual level, through feeding behavior and post-ingestive physiology, animals regulate their nutritional status, and therefore assimilation and homeostasis are nutrient-based. On the other hand, ecological stoichiometry focuses upon the elements themselves, e.g., **C**, **P**, and **N**. These elements represent an index of food quality rather than representing the full scope of processes determining dietary limitation. Ultimately, however, it is the mass of each element that is conserved and ecological stoichiometry seeks to resolve elemental concentrations by keeping track of the mass flow through the entire ecosystem, as it relates to both primary and secondary production. This view was expressed by Lotka (1925), and more recently by Sterner & Elser (2002).

A mathematical model for the individual could be based on either approach; both are supported by experiment. The approach we take is to observe that or-

ganisms themselves, and the food they consume, are made up of elements. Using a mass balance approach we account for these elements and formulate a tractable set of differential equations that models the mass fluxes through the system, where we treat the individual organism as a chemical reactor. It is less obvious how to resolve nutrient fluxes of the many complex macromolecules that make up the diet and the composition of the herbivore itself; e.g., a given ingested protein eventually disappears through its specific metabolic pathway. An elemental approach can also complement an experimental program where basic chemical elements (**C**, **N**, and **P**) of the food, the organism, and the egesta can be measured. This approach also allows linkage to other levels of biological organization, e.g., nutrient cycling in ecosystems. Other theoretical models have focused upon elemental, stoichiometric constraints as well, especially in predator-prey interactions and how elemental imbalances affect the underlying dynamics (Loladze et al 2000, Mueller et al 2001, Loladze et al 2003).

We show how modulation works in a three-nutrient system (**C**, **N**, **P**) and develop a model that controls consumer homeostasis through dynamic differential assimilation (Logan, Joern, & Wolesensky 2004a). A static, two-nutrient case (e.g., **C** and **P**) was studied by Sterner (1997) and Frost & Elser (2002). They show that the assumption of strict consumer homeostasis (constant **C:P** ratio) leads to an algebraic model of diet constraint relating food quantity and quality, and they define a homeostasis curve in food quality-quantity space that separates regions where consumer growth is **C**-limited (too little carbon) and where it is **P**-limited (too little phosphorus). To maintain a constant consumer **C:P** ratio, the consumer's diet must be confined to the curve. A two-dimensional dynamic model developed by Logan, Joern & Wolesensky (2004b) uses differential assimilation to control assimilation of elements to maintain the consumer **C:P** or **C:N** ratio within a tolerance envelope, even when the food supply is variable and time-dependent. Below, we illustrate a static case by defining a strict homeostasic curve in food CNP space relating food quantity, measured by carbon content times ingestion rate, and two quality variables defined by food **C:P** and **C:N** ratios. An alternate visualization to a three-element homeostasis representation is given by Thingstad (1987), whose static model for bacteria relaxes the condition of strict homeostasis, and elemental homeostasis is represented by regions in a two-dimensional space with axes **C:N** and **C:P**, both relating to the food supply. Also see Sterner & Elser (2002), p195. Secondly, we introduce the dynamic notion of differential assimilation control to maintain consumer **C:P** and **C:N** ratios simultaneously within a set tolerance range, even when the food quality and quantity leave the homeostasis curve and are time-dependent. When food has an extreme imbalance, control of elemental assimilation shuts down absorption of the over-abundant element(s) and subsequently restricts growth in **C**-, **P**-, or **N** -limited regimes. The model is based upon a dynamic environment and dynamic responses by the consumer while relaxing the condition of strict homeostasis.

An important related issue is where and how homeostasis is maintained in a herbivore? The answer to this question is not known completely. Three tactics that have been conjectured and studied are: selecting different foods when available, regulating assimilation of a given element or nutrient, and excreting excess elements through metabolism. We focus on one mechanism for the post-ingestive response, namely differential assimilation of elements. We interpret "differential assimilation" for an individual consumer in a broad sense, meaning assimilation in its entire system. We build a conceptual framework for homeostasis maintenance in the classical approach of mathematical modeling, where, as described in the last

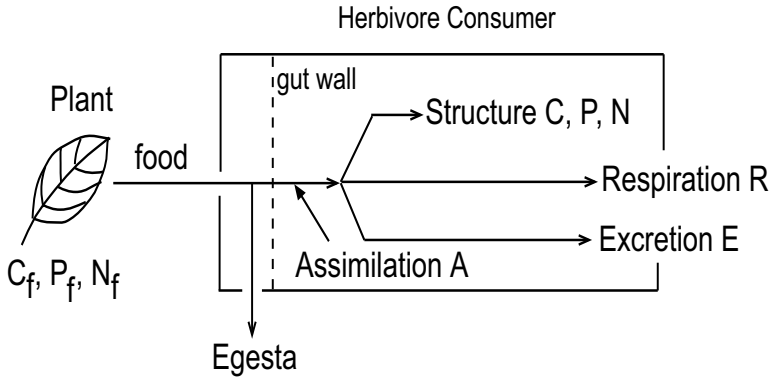

Figure 5: Elemental fluxes in a herbivore and its energy budget. Each element is ingested and a fraction is assimilated across the gut wall, the remaining being egested. The assimilated elements are distributed to structure (total biomass) and maintenance (respiration and excretion).

section, we ignore many of the intermediate details of precise biochemical processes. We do not include processes like pH or water control, both of which may play a role in insect digestion modulation. Also, we assume that the herbivore is in stages prior to maturity, and so we ignore energy currency explicitly allocated to reproduction (although one could consider some allocation to reproduction as built into production). We also do not consider storage.

In many insect herbivores (as well as other for many other taxa) there are three nutrients (**C**, **P**, and **N**) that affect growth, metabolism, and the maintenance of homeostasis. The structure of the model, set up as a chemical reactor, is shown in figure 5. The herbivore ingests food consisting of specific **C:N** and **C:P** ratios; some nutrients are egested, and some are assimilated across the gut wall for growth (production) and basal maintenance (respiration and excretion). For each element, we have following balance law for the fluxes:

$$\text{Per capita production} \;=\; \text{assimilation} \;-\; \text{respiration} \;-\; \text{excretion}$$

The model deals with three specific elements in the food and in the herbivore. The carbon biomass of the consumer is used to determine the per capita amount of **C**, **N**, and **P** required in the production and metabolism processes. **C** from the plants is used by consumers for both growth and maintenance (e.g., respiration through the loss of $\mathbf{CO}_2$), while **P** is used only for production. Although phosphorus is required in the biochemical pathways for metabolism, it is not generally lost through either excretion or respiration. **N** is used for production and it is often excreted as a by-product of metabolism, but not lost in respiration. Indigestible celluose in the food is accounted for in the fraction of food not assimilated, and hence egested.

To formulate model equations we use upper case italic letters to denote the elemental amounts of **C**, **N**, and **P**; thus $C = C(t)$, $N = N(t)$, and $P = P(t)$ denote consumer elemental biomasses (in moles); the subscript f on these quantities, e.g., $C_f = C_f(t)$, denotes the density (moles per volume) of the element in the food. We take g as the constant grazing (input) rate (volume per moles of **C** per time), and we let a_c, a_p, and a_n denote the constant (for present), dimensionless assimilations of the elements. The assumption of a constant feeding rate g is part of the steady-state

analysis; but the feeding rate can be time dependent. Some herbivores do maintain constant rates, but others exhibit compensatory feeding and increase feeding when food quality decreases. Finally, let m denote the constant respiration rate of **C** , and k the constant excretion rate for **N**, both given in time^{-1}. An obvious deficiency in the model we formulate is that m and k do not depend upon the food densities (see Gurney & Nisbet, 1998); however, the model can be extended to cover this case by letting m and k depend upon food intake. Another simplifying mathematical assumption is that the **N** excretion rate is constant and does not depend upon total **C** biomass; over long times, where there is significant growth, our assumption is invalid.

The basic **CNP** model can be written as

$$\frac{1}{C}\frac{dC}{dt} = gC_f a_c - m, \quad \frac{1}{C}\frac{dP}{dt} = gP_f a_p, \quad \frac{1}{C}\frac{dN}{dt} = gN_f a_n - k\frac{N}{C}, \tag{6}$$

Frost and Elser (2002), who consider just the two elements **C** and **P**, replace the ingestion rates $gC_f a_c$ and $gP_f a_p$ by saturating functions (Holling type II responses) of food densities to take account of handling time.

The term *homeostasis* is used in the sense defined by Kooijman (1995), i.e., the composition of the consumer is constant, regardless of the composition of the ingested food. We call this *strict homeostasis*; later we relax the constancy condition and only require homestasis within a restricted tolerance range. At present, for the herbivore consumer we assume $C/P = \beta$ and $C/N = \gamma$. Generally, $\beta > \gamma$ because herbivores contain much more **N** than **P**. Eliminating P and N from (6) yields two conditions for strict homeostasis,

$$gC_f a_c - m = \beta gP_f a_p = \gamma gN_f a_n - k. \tag{7}$$

We can introduce two food qualities, $Q_p = P_f/C_f$ and $Q_N = N_f/C_f$, which are the **P:C** and **N:C** ratios in the food. Equations (7) define a homeostasis curve in three-dimensional $Q_pQ_NC_f$–space that that can be represented as the intersection of two surfaces S_P and S_N defined by

$$S_P: \quad Q_p = \frac{gC_f a_c - m}{\beta gC_f a_p}, \qquad S_N: \quad Q_N = \frac{gC_f a_n + k - m}{\gamma gC_f a_n}. \tag{8}$$

The quantity gC_f on the right sides of (8) is a measure of the total quantity of food ingested, so that equations (8) represent quality *vs.* quantity surfaces of the ingested food. Referring to figure 6, a consumer must have a diet that lies on the curve AB to be in strict homeostasis. Near location B on the curve the food quantity is high and growth is high; near A, the lower end of the curve, growth is less. Observe that point A is limiting for growth since the homeostasis curve must lie in the positive octant, and this lower limitation depends upon the non-excreted mineral **P**, since $x > w$ (i.e., $m - k < m$), and since A lies on the intersection of the S_P surface with the coordinate plane. This conclusion is consistent with intuition; if a mineral is excreted (in this case **N**), then less **C** is required in the food to maintain homeostasis because that mineral is lost to production. So growth limitation will depend on the non-excreted mineral, where more **C** will be required to maintain homeostasis. Below each surface, respectively, the food is limited in that mineral, **P** or **N**. In the region that lies below both surfaces, both minerals are limited. Above the surfaces **C** is limiting (the food is high quality but the quantity, measured in the currency **C**, is small).

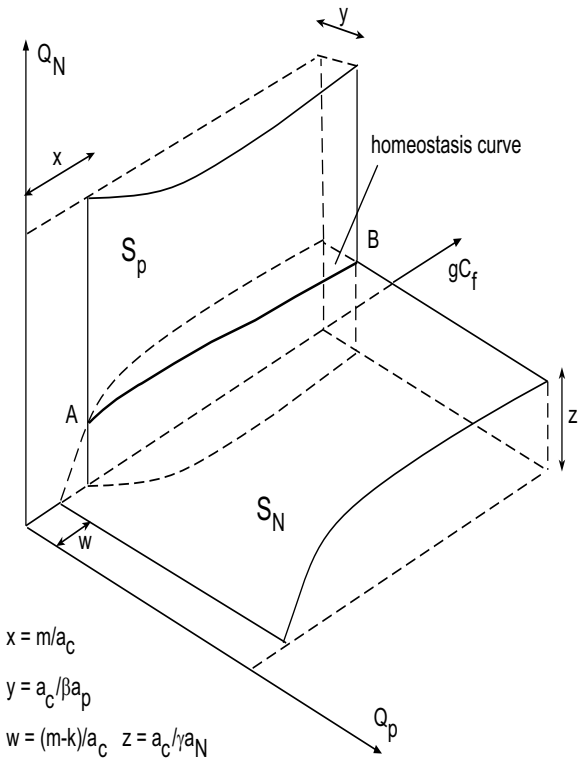

Figure 6: The homoestasis curve as the intersection of the quality vs. quantity surfaces.

.

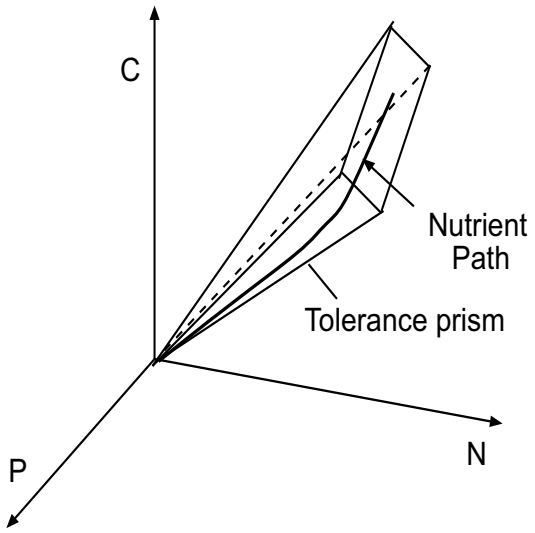

Figure 7: Schematic showing a typical herbivore response to a variable food supply in CNP space. Differential assimilation confines nutrient path to a tolerance prism containing strict homeostasis. In the interior, **C**, **N**, and **P** are assimilated at maximum rates. On a boundary (side or edge) one or more elements is limited.

4.1 Differential Assimilation

A static model does not indicate what will occur under variable environmental conditions, or what the consumer response is. There are many strategies a consumer can adopt when faced with food scarcity or low food quality. It often compensates by altering digestive tactics to meet its nutritional needs (Zanotto et al. 1993, Karasov & Hume 1997, Woods & Kingsolver 1999, Whelan & Schmidt 2003). Such tactics may include changing its morphology (e.g., gut size), changing the residence time of the food to maximize total uptake, or modifying absorption rates (Sibly, 1980, Dade *et al.* 1990, Martínez del Rio & Karasov 1990, Simpson & Raubenheimer 1993a; Yang & Joern 1994; Belovsky 1997, Jumars & Martínez del Rio 1999, Jumars, 2000a, Whelen & Schmidt 2003, Logan *et al.* 2002, 2003; Wolesensky 2002; Wolesensky *et al.* 2004). However, as we noted, how an animal actually regulates homeostasis is an open question. There is evidence that some animals modulate digestion by differential assimilation across the gut wall (Zanotto *et al* 1993, Woods & Kingsolver 1999). This is the response we model.

Rather than require exact homeostasis where the **C:N** and **C:P** ratios are strict constants, we assume that an organism will operate within a narrow tolerance zone defined by

$$\beta - \sigma \leq \frac{C}{P} \leq \beta + \sigma, \qquad \gamma - \epsilon \leq \frac{C}{N} \leq \gamma + \epsilon, \tag{9}$$

where σ and ϵ are tolerance ratios. These inequalities define a region in three-dimensional CNP space having the shape of a four-sided pointed prism (see figure 7). Our assumptions automatically define a homeostatic ratio for **N:P**; if a different **N:P** ratio is required by the consumer, then the tolerance zone would form a six-sided pointed prism (with an accompanying more complicated set of assimilation

rules than we give below for an automatically determined **N:P** ratio). Initially ($t = 0$) we assume the herbivore is in strict homeostasis, i.e.,

$$\frac{C(0)}{P(0)} = \beta, \qquad \frac{C(0)}{N(0)} = \gamma,$$

where $C(0)$ is the initial carbon biomass of the consumer. Then the elemental dynamics are governed by the system (6); the calculated values $C(t)$, $N(t)$, and $P(t)$ define a curve in CNP space called the elemental *nutrient path*, which is the trajectory of the consumer's stoichiometry. As long as the consumer's **C:N** and **C:P** ratios lie in the ranges defined by (9), i.e., its nutrient path lies in the tolerance prism, it assimilates all three elements at maximum constant rates, a_c^*, a_p^*, and a_n^* , to maximize growth. However, when food imbalance forces the nutrient path to a boundary of the prism (where equality holds in one or more cases in (9)), absorption of the excess element or elements is reduced so that the ratio remains in the prism, or on its boundary. For example, when a food is high in **C** and low in **N**, it is of low quality, and the nutrient path will be driven so as to track along the upper **C:N** boundary where assimilation of **C** is restricted; this is **N** -limited growth. Thus the assimilation 'constants' a_c, a_p, and a_n in the dynamic equations (6) become nonlinear functions of the carbon to mineral ratios. Rather than write out these functional relations specifically as single, complicated formulas, we define the assimilation rates piecewise in several cases.

To determine the appropriate assimilation rates to remain in the tolerance prism when one or both ratios reach a boundary, we solve an algebraic problem that comes from aligning the vector field of (6), at any time, on the boundary of the prism (either along a plane or an edge). There are eight cases to consider. The first four arise when the nutrient path reaches a bounding plane of the tolerence prism, and the last four cases occur when two planar boundaries are reached simultaneously, i.e., an edge is reached. We conveniently represent the dynamics in two 2-dimensional phase planes, the PC plane and the NC plane. The projection of the 3-dimensional tolerance prism onto those planes give triangular tolerance zones defined by (9).

We now enumerate the assimilation rules:

Case 1. When the upper boundary of the **C:P** tolerance prism is reached, i.e., $\frac{C}{P} = \beta + \sigma$, $\gamma - \epsilon < \frac{C}{N} < \gamma + \epsilon$, the consumer maintains maximum **P** and **N** assimilation rates ($a_p = a_p^*$, $a_n = a_n^*$) and restricts its **C** assimilation rate a_c such that the **C:P** ratio remains on the boundary. The vector field constraint $dC/dP = \beta + \sigma$ results in the algebraic condition

$$\frac{gC_f a_c - m}{gP_f a_p^*} = \beta + \sigma, \quad \text{or} \quad a_c = \frac{(\beta + \sigma) gP_f a_p^* + m}{gC_f}., \tag{10}$$

which determines the reduced carbon assimilation rate a_c. One can verify that $a_c < a_c^*$.

Case 2. When the lower boundary of the **C:P** ratio is reached, or $\frac{C}{P} = \beta - \sigma$, $\gamma - \epsilon < \frac{C}{N} < \gamma + \epsilon$, the consumer maintains maximum **C** and **N** assimilation rates ($a_c = a_c^*$, and $a_n = a_n^*$), while restricting a_p. The vector field constraint is $dC/dP = \beta - \sigma$, which gives

$$\frac{gC_f a_c^* - m}{gP_f a_p} = \beta - \sigma, \quad \text{or} \quad a_p = \frac{gC_f a_c^* - m}{(\beta - \sigma) gP_f}. \tag{11}$$

Case 3. When the **C:N** ratio reaches the upper boundary of its tolerance zone, but the **C:P** ratio remains with in its respective zone, $\beta - \sigma < \frac{C}{P} < \beta + \sigma$, $\frac{C}{N} = \gamma + \epsilon$, the consumer maintains maximum **P** and **N** assimilation ($a_p = a_p^*$, and $a_n = a_n^*$) and restricts a_c via

$$\frac{(gC_f a_c - m)C}{gN_f a_n^* C - kN} = \gamma + \epsilon, \quad \text{or} \quad a_c = \frac{(\gamma + \epsilon)gN_f a_n^* - k + m}{gC_f}. \tag{12}$$

Case 4. The final single boundary case occurs when the **C:N** ratio reaches the lower boundary of its tolerance zone and **C:P** remains within its tolerance zone, or $\beta - \sigma < \frac{C}{P} < \beta + \sigma$, $\gamma - \epsilon = \frac{C}{N}$. The maximum assimilation rates are adopted for both **C** and **P** ($a_c = a_c^*$, $a_p = a_p^*$) but a_n is limited via the condition

$$\frac{(gC_f a_c^* - m)C}{gN_f a_n C - kN} = \gamma - \epsilon, \quad \text{or} \quad a_n = \frac{gC_f a_c^* - m + k}{gN_f(\gamma - \epsilon)}. \tag{13}$$

Case 5. The next four cases occur when both ratios **C:N** and **C:P** reach the boundaries of their envelopes simultaneously (i.e., the nutrient path reaches an edge of the prism). First consider $\frac{C}{P} = \beta - \sigma$, $\frac{C}{N} = \gamma - \epsilon$. Both ratios allow maximum assimilation for carbon ($a_c = a_c^*$), but **N** and **P** are limited The conditions that determine a_n and a_p are given by (11) and (13). These two conditions are independent and yield (13) and (11) for a_n and a_p, respectively.

Case 6. When $\frac{C}{P} = \beta + \sigma$, $\frac{C}{N} = \gamma + \epsilon$, assimilation rates for **P** and **N** remain maximal ($a_p = a_p^*$, $a_n = a_n^*$), but the assimilation rate for **C** is determined by (10) and (12). For both the **C:P** and **C:N** ratios to remain in their respective tolerance zones we choose a_c to be the minimum of (10) and (12).

Case 7. When

$$\frac{C}{P} = \beta + \sigma, \qquad \frac{C}{N} = \gamma - \epsilon, \tag{14}$$

the ratios permit maximum assimilation of **P** ($a_p = a_p^*$), but require a_c and a_n to be restricted. Using the constraints $dC/dP = \beta + \sigma$ and $dC/dN = \gamma - \epsilon$ we obtain the conditions

$$\frac{gC_f a_c - m}{gP_f a_p^*} = \beta + \sigma, \qquad \frac{(gC_f a_c - m)C}{gN_f a_n C - kN} = \gamma - \epsilon. \tag{15}$$

The consumer can maintain elemental homeostasis by remaining on the two boundaries given in (14). The algebraic equations given in (15) uniquely determine the two assimilation rates, a_c and a_n given by

$$a_c = \frac{(\beta + \sigma)gP_f a_p^* + m}{gC_f}, \qquad a_n = \frac{(\beta + \sigma)gP_f a_p^* + k}{gN_f(\gamma - \epsilon).}$$

Case 8. The final case is

$$\frac{C}{P} = \beta - \sigma, \qquad \frac{C}{N} = \gamma + \epsilon. \tag{16}$$

The assimilation rate for **N** is unrestricted ($a_n = a_n^*$) and we can proceed as in Case 7. The homeostasis conditions are

$$\frac{gC_f a_c - m}{gP_f a_p} = \beta - \sigma, \qquad \frac{(gC_f a_c - m)C}{gN_f a_n^* C - kN} = \gamma + \epsilon. \tag{17}$$

We uniquely determine assimilation rates for **C** and **P** that allow the ratios **C:P** and **C:N** to remain on the boundaries (16). Solving (17) gives

$$a_c = \frac{(\gamma+\epsilon)gN_f a_n^* - k + m}{gC_f}\ , \qquad a_p = \frac{(\gamma+\epsilon)gN_f a_n^* - k}{(\beta-\sigma)gP_f}.$$

To summarize, the mathematical model consists of the dynamical equations (6) subject to the constraining relationships defined in Cases 1–8. The nutrient path $C = C(t)$, $N = N(t)$, $P = P(t)$ in CNP space begins at an initial homoestatic state and then moves through the tolerance prism. Within the interior of the prism all nutrients are assimilated at their maximum rates a_c^*, a_p^*, and a_n^*. If the food supply drives the nutrient path to the boundary of the prism, then the assimilation rates are selected to align the vector field of (6) along that boundary so that it does not escape the prism. Physiologically, the herbivore differentially assimilates; when the food supply is extreme, it will operate at the edge of its tolerance range, thus limiting its production, and therefore its growth, in one or more nutrients. Maximum growth will occur when the food supply is such that the nutrient path remains near exact homeostasis, i.e., when it most matches the chemical composition of the consumer itself.

This model is consistent with Leibig's law of the minimum, which states that a growth will be limited by whichever single resource is in lowest abundance in its environment, relative to its needs. Although this rule is normally associated with plant growth, it is also applied to consumers (e.g., Thingstad 1987, Sterner & Elser 2002, p190ff). In the model above, either *one* or *two* nutrients can be limiting. In the latter case, for example, a food supply low in **N** and low in **P** can drive the nutrient path to an edge of the tolerance region (Case 6) where the consumer strongly limits its **C** assimilation to maintain two homeostatic ratios. Thus Leibig's rule requires a more general interpretation to allow for multiple limiting nutrients (see Bloom *et al* 1985).

4.2 Numerical Simulations

We can turn to simulation to solve the differential equations (6) numerically, subject to the controls defined in Cases 1–8. Because the model can describe many scenarios, a large number of computations could be performed to illustrate results for different food inputs (food qualities, food quantities, grazing rates), different maximum assimilation rates (depending upon taxa), and different tolerance ratios. For each variation, total growth in **C**, **N**, **P**, the total amount of excreta and egesta returned to the environment, as well as the nutrient paths, can be calculated. To limit space, however, we illustrate how the model performs in a specific case.

Generally, experiments on three-element systems are lacking. In insect herbivores, for example, there is significant support of viewing **N** as a likely limiting nutrient (e.g., White 1993); but evidence for **P** is only now building and data are scarce (Sterner & Elser 2002). In grasshoppers, for example, availability of excess bulk food is the norm, but the capacity to find high quality **N** food is limiting; the role of **P** is not known. Generally, **C** comprises the bulk dry weight of organisms, and in terrestial organisms **P** is more variable than **N** (Sterner & Elser 2002). Thus, the variability in the **C:N** ratio is much less than in the **C:P** ratio. Many factors, e.g., different habitats, the presence of vacuoles, etc., force plants to have larger variations in their **C:P** ratios as well.

For a generic simulation we take median values of terrestial invertebrate **C:N** and **C:P** ratios catalogued by Sterner & Elser (2002, p 140ff), and typical plant

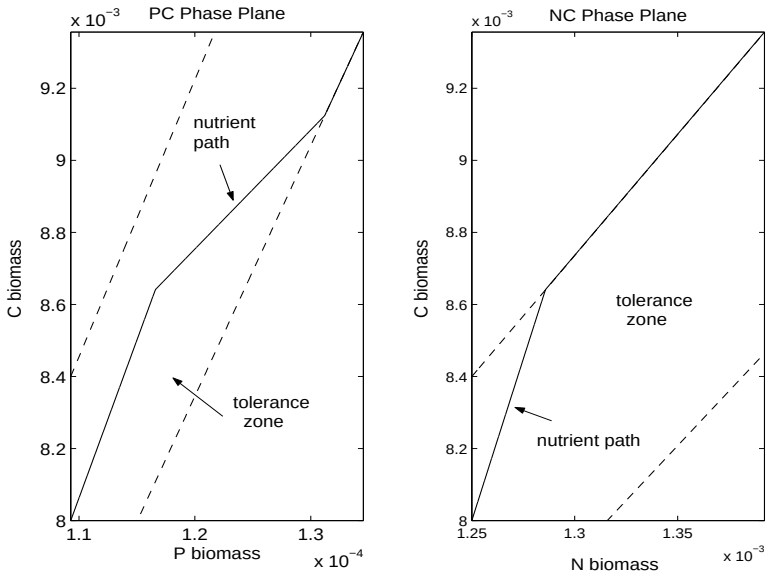

Figure 8: Simulation for 96 hours showing the nutrient paths in the two phase planes. The food supply is fixed with $C_f/P_f = 263$ and $C_f/N_f = 30$.

ratios (p 120 ff). Their tables show large variations in all these ratios. For the herbivore consumer we take **C:P** = 73.2 and **C:N** = 6.4, which leads to an **N:P** ratio of 11.4, well within observations in some taxa. The tolerance ratios σ and ϵ are chosen arbitrarily to be five percent of each ratio. For food we take C:P = 263 and **C:N** = 30. The total time of the simulation is 96 hrs, or 4 days. A typical grasshopper, for comparison, might require about three times this period to progress through one of its five instars. The other parameter values are provided in the accompanying table. These average values lead to interesting dynamics and illustrate the model's performance.

Quantity	**Name**	**Value**
g	*grazing rate*	0.001 l (mol **C**)$^{-1}$ hr^{-1}
m	**C** *respiration rate*	0.002 hr^{-1}
k	**N** *excretion rate*	0.0002 hr^{-1}
a_c^*	C *assimilation*	0.5
a_p^*	**P** *assimilation*	0.9
a_n^*	**N** *assimilation*	0.6
β	**C:P** *biomass ratio*	73.2
γ	**C:N** *biomass ratio*	6.4

The nutrient path is illustrated as two parametric paths in the PC-plane and the NC-plane (figure 8). One can favorably compare these types of plots to the experimental plots of Simpson & Raubenheimer (2000, p 29). At first, both **C:P** and **C:N** ratios are high because of high **C** concentration in the food (low quality). The nutrient path approaches both upper boundaries where **C** assimilation becomes reduced. Over time, however, the **C** limitation leads to excess **P** and drives the nutrient path toward the lower boundary of the **C:**P zone, while the **C:N** ratio

remains in excess, causing the path to track on the boundary on the **C:N** zone. After a time the path reaches the boundary of the **C:P** zone and thus assimilation of **P** is restricted. The system continues then to track along the tolerance boundaries where both **C** and **P** are limited (**C** limited to maintain constant **C:N** and **P** limited to maintain constant **C:P**).

With regard to a regulatory physiological approach one could consider identifying **C** with carbohydrate and **N** with protein and plot curves on a protein-carbohydrate plane. We discuss this in the next section. In this model an organism responds to an extreme food supply by tracking along the boundaries (rather than the interior) of its nutrient thresholds. One or more elements will be limited and total production in that element will be limited, leading to restricted growth. If the food is well-matched to the herbivore, the path will track in the interior of its tolerance zones, leading to maximum assimilation of all the elements, and therefore maximum production. This model fits well, in concept, with the empirical conclusions of Simpson & Raubenheimer (2000). In experiments with locusts they found target ratios for different nutrients (e.g., protein vs. carbohydrate). This target ratio must lie in some domain in nutrient space for the organism to survive and advance to the next instar. Corresponding to a target zone there is a set of food nutrient ratios where the insect's nutrient path can reach its target zone. Although we do not pursue this here, the model has the capability of determining the domain of food elemental ratios that force the nutrient path into a given terminal set, some subregion of the tolerance prism.

From a number of simulations one can calculate the total percentage accumulation of **C**-biomass in the insect after 96 hours for different food qualities measured by the ratio N_f/C_f of the food. The carbon and phosphorus contents remain unchanged. Collective simulations show that as the nitrogen content increases, i.e., as the food becomes higher quality, the final **C**-biomass increases up to a limiting value (33.8%) at about $N_f/C_f = 0.07$; it then levels off, and no further growth occurs because at higher food quality the nutrient path remains in the interior of the tolerance prism for the 96-hour duration of the simulation.

One important issue is the time scale over which the model and its simulations are valid. We have given simulations in a short-to-intermediate time length of 96 hours where the food supply and ingestion rate are assumed to be constant. In reality, over this physiological time scale the food rail could be quite erratic with intervals of no ingestion and changing food composition, resulting in the animal constantly switching its nutrient path back and forth in the prism. Over long, developmental, time scales the food quality can vary significantly over a season; for example, the nitrogen content of plants can decrease dramatically over the summer, leading to an increasing **C:N** food ratio over time. The model can accommodate these variations by inputting g, C_f, P_f, and N_f as functions of time, or even including stochastic effects of weather. Yet one qualification remains. Over developmental time scales, where growth is significant, the linearity and the density-independent assumptions in the model equations (6) may lose some of their validity. Over shorter, physiological time scales, the model may perform better in predicting growth. To adapt the ecological-stochiometric model as a link in the overall nutrient cycling problem in an ecosystem require modifications that account for these nonlinearities. For example, the **N** excretion rate k may depend upon total consumer **C**-biomass. And, the role of temperature, which is especially significant for insects, must ultimately be included in the model as a factor that affects absorption rates and metabolic activity (e.g., Wolesensky 2002, Wolesensky *et al* 2004). Temperature is included in the regulatory model below.

To summarize the model, host plants provide complex and variable concentrations of elemental nutrients. Growing herbivores face the problem of having to manage multiple and changing nutrient needs in a multidimensional and variable nutrient environment. We have incorporated differential assimilation to control elemental homeostasis in a consumer eating food of significantly different elemental ratios. The model includes variable food input and variable grazing rates. By including a tolerance zone around strict homeostatic control, we show that a herbivore consumer can adjust its assimilation in response to limiting elements in its diet. As food supply ratios change, independent of the actions of the consumer, assimilation changes accordingly and relative elemental accumulation shifts. Thus, differential assimilation can effectively act as a nonlinear control mechanism permitting elemental homeostasis in consumers, as predicted by Sterner (1997). Under variable conditions the model can predict total production, or growth, and in what regimes growth is **C**-, **P** -, and **N**-limited.

One important conclusion that can be deduced from several simulations is that assimilation rates may play an equal role to food supply ratios in maintaining homeostasis. Even in the case where the food ratios **C:N** and **C:P** are are exactly those of the homeostatic state of the consumer, the nutrient path may not track in the interior of the tolerance zone along the ideal path, but rather track on a boundary with one or more nutrients limited, thus limiting production. This limitation can be forced by changing the assimilation rates of the different elements. In insects, for example, variable assimilation rates may be the rule because digestion processes depend so strongly upon temperature. One important research question, both theoretically and experimentally, is to understand how temperature variations affect the assimilation rates of various nutrients and elements.

With appropriate qualifications we can view this model as one link in the overall nutrient cycling process in natural systems. It permits the calculation of secondary production, based on the composition of the food supply. Coupled with models for the other components of the nutrient cycle (e.g., DeAngelis 1992), it could form another piece of this overall stoichiometric process.

5 DIGESTION MODULATION IN GRASSHOPPERS

In this section we begin part two of the paper. We show how serially connected chemical reactors can be set up to effectively capture speicific behaviors associated with foraging and digestion. The discussion extends the model of Wolesensky *et al.* (2004) by expanding a crop-midgut-hemolymph (figure 9) model to include a multidimensional nutrient space and controls that reflect two compensatory behaviors that insects employ when faced with nutritionally incomplete food. In particular, we are interested in the qualitative organism responses with respect to variation of the nutritional quality of the diet.

The nutritional needs of insects, in particular grasshoppers, are best understood in the context of a multidimensional nutrient space (Simpson & Raubenheimer, 1993b; Simpson *et al.*, 2002; Lee *et al.*, 2002). To achieve optimal growth it is necessary for insects to ingest a variety of substrates in different ratios. Ideally, insects regulate their intake of the various nutrients needed for optimal growth by simply eating a mix of foods rather than a single food (Bernays & Bright, 1993; Simpson & Simpson, 1990; Simpson *et al*, 1995; Waldbauer and Friedman, 1991; Behmer & Joern, 1993). These include artificial foods that differ in nutrients such

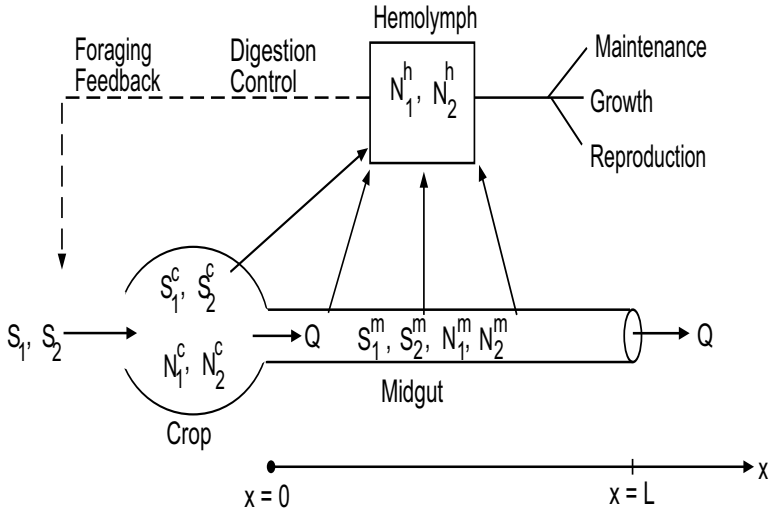

Figure 9: Schematic of alimentary system with feedbacks. Food is loaded instantaneously into the crop where a small amount of reaction and absorption occur as the digesta moves into the midgut. It passes through the midgut at a speed dependent on its quality; in the midgut it breaks down and the nutrient products are absorbed along its length into the hemolymph system. There, nutrients of concentration P_1^h and P_2^h are distributed to the grasshopper's energy needs; upper and lower threshold levels trigger the cessation and onset of feeding.

as protein and carbohydrate (Cohen *et al.*, 1987a,b; Chambers *et al.* 1995; Behmer *et al.*, 2001; Lee *et al.*, 2002). For example, given *ad-libitum* access to pairs of nutritionally complementary foods (foods that contain nutrients in ratios that allow an insect to optimally reach their required nutrient levels by alternating between the foods), *Locusta migratoria L.* nymphs have been observed to alternate between them and thus attain highly convergent nutrient intake across different food pairings (Chambers *et al.*, 1995; Behmer *et al.*, 2001).

For many insects plant foliage serves as their food-source. But plant foliage has many limitations when it comes to meeting nutritional goals. For example, most foliage is relatively low in protein and may also be low in digestible carbohydrate relative to nutritional needs (Bernays & Simpson, 1990). It has been suggested (Bernays & Simpson, 1990) that the consequences an insect faces when consuming food with nutritional deficiencies include: tolerate the deficiencies and pay the price of an extended development, reduced fecundity, and/or increased mortality; leave and attempt to find an alternate food supply; or compensate for the change. Many insects have developed mechanisms that allow them to compensate for nutritionally deficient food.

Two forms of compensation that we will incorporate into the mathematical model include (Bernays & Simpson, 1990): (i) Eating more or less of the same food until it meets the limiting nutritional requirement; (ii) Adapt its digestive and assimilatory physiology so that more or less efficient use is made of the ingested nutrient. Evidence of compensation in the form of (i) occurring in locust has been repeatedly reported (Raubenheimer & Simpson, 1993; Behmer *et al.*, 2001; Simpson *et al.*, 2002). Results showed that when a near optimal ratio of protein to carbohydrate was provided in the food, but the concentration was diluted across a fivefold range by addition of indigestible cellulose, the locusts adjusted their intake accordingly, eating five times as much of the dilute food as of the most concentrated. Experimental evidence of compensatory behavior (ii) was presented in Zanotto *et al.* (1993). They found that when fifth-stadium L. migratoria were fed foods limited in carbohydrate, they achieved "unjamming" of the regulatory mechanisms through selectively egesting lysine, an amino acid known to play a key role in signaling protein repletion.

Moreover, it has been suggested that both pre- and post-ingestive mechanisms (compensatory behaviors (i) and (ii), respectively) of nutritional homeostasis may be coordinated (Raubenheimer, 1992). This type of behavior is illustrated in the case when an animal stops feeding on a nutritionally unbalanced food due to negative feedbacks occurring from the nutrient(s) present in excess. This cessation of feeding could then result in the animal not ingesting sufficient amounts of other needed nutrients that occur in the food only at lesser levels. This animal would be well served by selectively increasing the egestion of the excess nutrient (Simpson & Simpson, 1990).

The mathematical model in the sequel simulates both pre- and post-ingestive changes that insects employ when faced with suboptimal foods. To understand the geometry of multidimensional nutrient space a very brief review of nutrient targets and rails follows. For a full discussion the reader is referred to Simpson & Raubenheimer (1995).

By viewing an insect as existing within a multidimensional nutrient environment we are able to define a geometry in which each axis represents a nutrient (or non-nutrient) compound found in foods. Within this nutrient space lies points which can be thought of as representing the animal's nutritional requirements. These points represent functional targets, and it is expected that animals will have developed

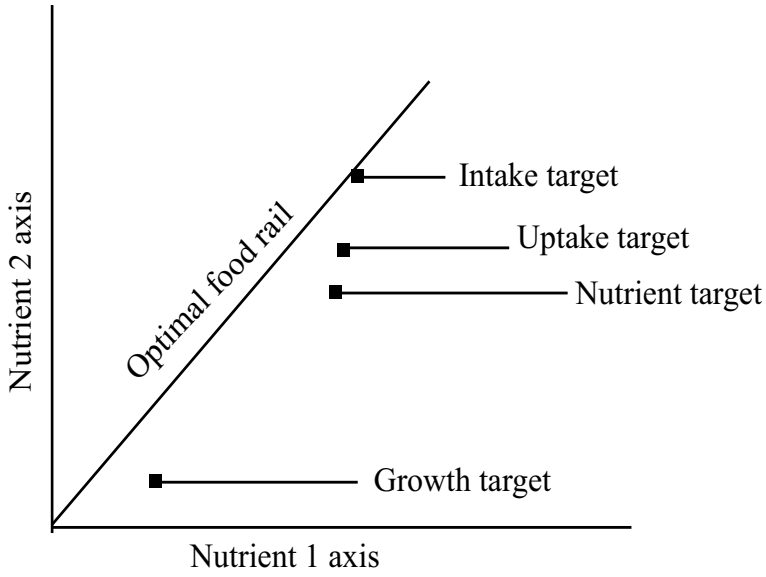

Figure 10: Plot showing various nutrient targets and their location relative to the optimal food rail. If an animal could operate at 100% digestive efficiency the intake target, nutrient target, and uptake target would correspond to the same point in nutrient space.

mechanisms that allow them to approach these points (Simpson & Raubenheimer, 1996, 2000). We can view targets as either static points, integrated over a given period of time, or as dynamic trajectories.

We extend the definitions given in Simpson & Raubenheimer (1995) by defining the uptake target. The uptake target represents the blend of nutrients absorbed into the hemolymph that will allow the animal to reach its nutrient target (the animals total nutritional requirement). If an animal were able to operate with complete efficiency when partitioning nutrients from the hemolymph for growth and metabolic needs, then the uptake target and nutrient target would be identical. The schematic in Figure 10 represents the relationship between the various targets. The distance that the uptake and nutrient target are from the intake target depends on how efficiently the animal processes ingested food.

Foods are mixtures of various nutrient and non-nutrient compounds and thus represent lines in our nutrient space that begin at the origin and extend into nutrient space. Simpson & Raubenheimer (1996, 2000) use the term rails for these lines because if an animal is confined to eating a single food then its is forced to ingest the ratio of nutrients that this food contains and thus stay on this single trajectory (or rail) in nutrient space. The animal can move along the rail into nutrient space by continuing to eat more of this food, and can get off this rail only by switching to another food or differentially utilizing nutrients post-ingestively (Simpson & Raubenheimer, 2000).

We can also use the information provided by our nutrient space to determine the animal's current nutritional state. The vector originating at the point that represents the animals current nutrient state and ending at the animals intake target indicates which nutrients need to be ingested if the animal is to reach its intake

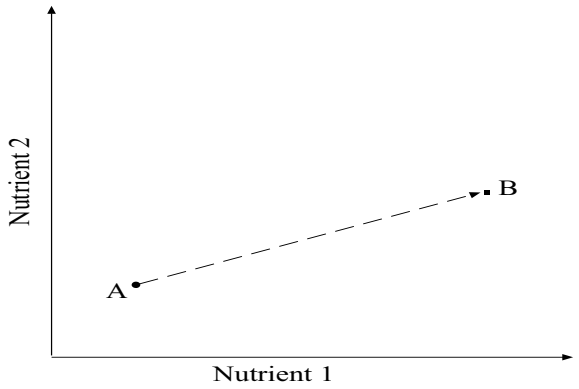

Figure 11: Vector from current nutritional state (A) to target (B) defines the nutritional quality of the optimal food (i.e. food that allows the insect to proceed directly to target).

target (Figure 11). If a food allows the animal to proceed directly along a rail to the intake target, then that food is defined to be an optimal food.

The following mathematical model is designed to simulate the behavior of an animal when confined to consuming a single suboptimal food. Although it is not possible for an animal to reach its uptake target when presented with a suboptimal food, it is important to note that it may still progress towards its various targets by making compensatory changes in its intermeal behavior and post-ingestive utilization of nutrients. The form of the post-ingestive compromise should depend on the relative weighting given by its regulatory systems to the nutrients involved (Simpson and Raubenheimer, 2000). Using a chemical reactor model for digestion, we invoke a post-ingestive control that allows the animal to proceed toward their uptake target by limiting the absorption of the nutrient that is in excess. We also make a pre-ingestive change by having the intermeal delay shortened if one of the nutrients occurs at a diluted level.

We now consider the case where the ingested food contains two substrates that react with enzymes to produce two nutrient products. That is, $\mathbf{S}_1 + \mathbf{E}_1 \rightarrow \mathbf{N}_1$ and $\mathbf{S}_2 + \mathbf{E}_2 \rightarrow \mathbf{N}_2$. We include a control to simulate post-ingestive changes, and we use Michaelis-Menten kinetics for the uptake of nutrient products into the hemolymph. Superscripts denote the structure being considered (c - *crop*, m - *midgut*, h - *hemolymph*) and subscripts denote the quantities associated with the reaction ($i = 1$ or $i = 2$).

5.1 The Crop

The function of the crop in the model is twofold. First, the crop regulates the quantity of food ingested during each meal. We assume a fixed volume of food V_0 enters the crop each time a meal is consumed, and then empties at a rate Q_n dependent upon food quality and the external temperature. Second, there is substrate reaction and very limited nutrient absorption in the crop; as is the case with for many insects, the degree of reaction and absorption is small compared to that occurring in the midgut (Srivastava, 1973; Wigglesworth, 1984). We model the crop as a semi-BR emptying at volumetric flow rate Q_n, which is determined in the model

at the time the nth meal is ingested. The flow rate Q_n remains constant until the crop empties, at which time it becomes 0; then at the instant $t = t_{n+1}$, when the $(n+1)$st meal is ingested, the flow rate Q_{n+1} is again determined and the cycle repeats. The determination of the flow rate Q_n, which depends upon food quality, is discussed in the sequel. For substrates we use W_i^c, and K_i^c, $i = 1, 2$, to denote the Michaelis-Menten constants for the maximum reaction velocity and concentration to half maximum velocity (half-saturation), respectively. Likewise, J_i^c and M_i^c, $1, 2$, denote the Michaelis-Menten constants for the absorption of the nutrients across the crop lining. Letting $t_e = V_0/Q_n$ (time for crop to empty), we apply mass balance to both substrate and nutrient in the crop during the time interval $(t_n,\, t_{n+1})$ to obtain

$$\begin{aligned} \frac{dS_i^c}{dt} &= -\left(\frac{W_i^c S_i^c}{K_i^c + S_i^c}\right) 2^{\frac{(\theta-\theta_o)}{10}}, \quad S_i^c(t_n) = S_i^n, \quad V(t) \neq 0, && (18)\\ S_i^c(t) &= 0,\ V(t) = 0, && (19) \end{aligned}$$

$$\begin{aligned} \frac{dN_i^c}{dt} &= \left[\left(\frac{W_i^c S_i^c}{K_i^c + S_i^c}\right) - \left(\frac{J_i^c N_i^c}{M_i^c + N_i^c}\right)\right] 2^{\frac{(\theta-\theta_o)}{10}}, \quad N_i^c(t_n) = 0, \quad V(t) \neq 0, && (20)\\ N_i^c(t) &= 0, \quad V(t) = 0, && (21) \end{aligned}$$

$$\begin{aligned} V(t) &= V_0 - Q_n(t - t_n), \quad t_n \leq t < t_e, && (22)\\ V\,(t) &= 0, \quad t_e \leq t < t_{n+1}. && (23) \end{aligned}$$

Observe that both the reaction and absorption terms depend on the concentrations as well as the external temperature $\theta = \theta(t)$. It is well-recognized that temperature plays a vital role in the thermal regulation of digestion in insects (Hoffman, 1984; Karasov, 1988; Chappel & Whitman, 1990). We incorporate temperature into these rates using $Q_{10} = 2$ (i.e., rates double for every 10°-temperature increase; Hoffman, 1984; Karasov, 1988;). Although Q_{10} may vary significantly for different processes (Harrison & Fewell, 1995; Gilbert & Raworth, 1996), for simplicity we assume it to be equal to 2 for all processes. The daily temperature cycle is modeled by the periodic function $\theta = \theta_0 + A_\theta \cos(\omega t)$, where $\omega = \pi/12$ and A_θ is the amplitude variation around the value θ_0.

5.2 The Midgut

We model the midgut as a PFR and obtain through mass balance the following coupled system of reaction–advection equations governing the concentrations of the substrate and nutrient as the bolus travels through the midgut

$$\begin{aligned} \frac{\partial S_i^m}{\partial t} + C_n \frac{\partial S_i^m}{\partial x} &= -\left(\frac{W_i^m S_i^m}{K_i^m + S_i^m}\right) 2^{(\theta-\theta_o)/10}, && (24)\\ S_i^m(x,0) &= 0, \quad S_i^m(0,t) = S_i^c(t), && (25) \end{aligned}$$

$$\begin{aligned} \frac{\partial N_i^m}{\partial t} + C_n \frac{\partial N_i^m}{\partial x} &= \left[\left(\frac{W_i^m S_i^m}{K_i^m + S_i^m}\right) - \left(\frac{J_i^m N_i^m}{M_i^m + N_i^m}\right) R_i\right] 2^{(\theta-\theta_o)/10}, && (26)\\ N_i^m(x,0) &= 0, \quad N_i^m(0,t) = N_i^c(t). && (27) \end{aligned}$$

We have included a control R_i in equation (26) that depends on the ratio of the nutrient products, N_1^h and N_2^h, in the hemolymph at the time a meal is consumed. It operates under the assumption that the optimal intake of the two nutrients is a 1:1 ratio, as is approximately the case for protein and digestible carbohydrate in locusts (Chambers *et al.*, 1995), but is readily adjustable for other required homeostatic ratios. We use the simple relationships

$$R_1 = \begin{cases} 1, & \text{if } N_1^h(t_n) \le N_2^h(t_n), \\ \frac{N_2^h(t_n)}{N_1^h(t_n)}, & \text{if } N_1^h(t_n) > N_2^h(t_n), \end{cases}, \tag{28}$$

and

$$R_2 = \begin{cases} 1, & \text{if } N_2^h(t_n) \le N_1^h(t_n), \\ \frac{N_1^h(t_n)}{N_2^h(t_n)}, & \text{if } N_2^h(t_n) > N_1^h(t_n). \end{cases} \tag{29}$$

5.3 The Hemolymph

The two nutrients products $\mathbf{N}_1$ and $\mathbf{N}_2$ are absorbed into the hemolymph from both the crop and midgut. Treating the hemolymph as a CSTR and applying mass balance, we obtain equations for the nutrient concentrations N_1^h and N_2^h in the hemolymph. For N_i^h we have

$$\begin{aligned} V^h \frac{dN_i^h}{dt} &= A\int_0^L \left(\frac{J_i^m N_i^m}{M_i^m + N_i^m}\right) 2^{(\theta-\theta_o)/10} \times R_i \, dx + \\ &\quad V(t)\left(\frac{J_i^c N_i^c}{M_i^c + N_i^c}\right) 2^{(\theta-\theta_o)/10} - V^h \lambda_i^h N_i^h 2^{(\theta-\theta_o)/10} - d_i, \\ N_i^h(0) &= N_{i_0}^h. \end{aligned} \tag{30}$$

We note that the inclusion of a non-local (integral) term is a result of absorption ocurring over the entire length of the midgut.

5.4 Feedbacks and flow-through speed

There is strong experimental evidence that nutrient titers in the hemolymph provide nutrient-specific influences on feeding behavior in several species of acridids and caterpillars (Abisgold & Simpson, 1987; Simpson & Simpson, 1990, Simpson & Raubenheimer, 1993a). From empirical evidence Simpson & Raubenheimer (1993a) conclude that hemolymph parameters, such as nutrient titers, are linked with the gustatory responsiveness of the insect. In particular, they noted that: (1) insects with low concentrations of particular nutrients in the hemolymph (nutrient deficient) were more likely to locomote and forage for food than those insects that are nutritionally replete, and (2) high concentrations in the hemolymph of certain nutrients will inhibit further feeding on food containing that nutrient. We integrate these observations into the model by defining upper and lower thresholds of the nutrient concentrations in the hemolymph that either increase or decrease the gustatory responsiveness of the animal. We extend the idea presented in Wolesensky *et al* (2004) to two nutrients by assuming upper thresholds, U_h^1, and U_h^2, and lower thresholds, U_l^1 and U_l^2, for the concentration of nutrients $\mathbf{N}_1$ and $\mathbf{N}_2$, respectively. We then use the following rules to determine the gustatory response in the model:

1. If both nutrient concentrations in the hemolymph exceed their respective upper thresholds (U_h^1, U_h^2) then the gustatory response is turned off (the simulated insect will cease to eat).

2. Gustatory response will remain off until the time when one of the nutrient titers in the hemolymph drops below its lower threshold (U_l^1, U_l^2). Then gustatory response is restored and the simulated insect is now hungry.

3. Feeding responsiveness will remain high until both nutrient concentrations again exceed their upper thresholds.

Rule 3 allows for feeding to continue until the upper threshold of the limited nutrient is reached in the hemolymph, regardless of how much excess nutrient is consumed (Simpson & Raubenheimer, 1995). Note that the hemolymph feedback described has the effect of delaying the onset of the next meal if high quality food is ingested. This is consistent with experimental work involving grasshoppers (Yang & Joern, 1994; Simpson & Raubenheimer, 2000). During the period where nutrient levels are satisfactory, in between the threshold values, we assume that quiescent or foraging behavior may be occurring. Foraging behavior is simulated by selecting a foraging time, which is an exponentially distributed random variable R_e; i.e., $\Pr(R_e \leq t) = 1 - \exp(-\eta t)$ (e.g., see Gross, 1986), where η^{-1} is the average foraging time. We incorporate dietary dilution of a substrate in the food by using a dilution factor D_f that depends on the ratio of the limited substrate concentration (corresponding to limited nutrient in the hemolymph) in the suboptimal food compared to the concentration of this substrate in the optimal food. For example, suppose it is determined that a food containing 14% protein and 14% digestible carbohydrate is optimal, but the animal is presented with a single suboptimal food containing only 7% protein and 14% digestible carbohydrate. In this case we would then have $D_f = \frac{.07}{.14} = .5$ and the foraging delay would then be half of what is required for optimal foods. This behavior has been exhibited by a variety of insects, including grasshoppers. McGinnis & Kasting (1967) reported that when fifth-instar nymphs of *Melanoplus sanguinipes*(grasshoppers) were fed a diet of wheat sprout meal diluted to various degrees with cellulose, they adjusted according to the amount of dilution. They observed that when these grasshoppers had the sprout meal diluted by two-, four-, and eight-fold, consumption over the first 5 days of the stadium increased by 2, 4, and 7 times respectively. The change in food consumption was not due to larger meals, but instead the compensation came from the insects eating the same size meals more frequently (Simpson & Simpson, 1990).

We make flow through speed dependent on food quality (Yang & Joern 1994),and determine the speed of material through the midgut using the concentration of the substrate that corresponds to the limiting nutrient (the nutrient which the animal is deficient). For example, if at time t_n the concentration of nutrient N_1^h is less than N_2^h, we use $S_n^c = S_1^c(t_n)$ when computing the contribution of the n^{th} meal to the midgut speed. Thus S_n^c denotes the substrate concentration that corresponds to the limiting nutrient at the time that the n^{th} meal is eaten. We formulate the contribution of the n^{th} meal in determining the midgut speed by

$$F_n = F(S_n^c) = w_n \frac{LW^m}{K^m + S_n^c}. \tag{31}$$

Here w_n represents the weight given to the n^{th} meal, while W^m and K^m are the midgut Michaelis–Menten constants for the substrate S_n^c. The midgut speed is then

computed using a weighted average of the meals that still *remain* in the midgut at the time the n^{th} meal is consumed; that is

$$C_n = [w_n F(S_n^c) + w_{n-1} F(S_{n-1}^c) + w_{n-2} F(S_{n-2}^c) + ... + w_{n-k} F(S_{n-k}^c)]. \quad (32)$$

This formula is purely theoretical in nature, but it exhibits the response observed empirically (Yang & Joern, 1994) that high quality food passes through the midgut at a slower rate than low quality food. This formula also has the advantage that it takes into account the "digestibility" of the substrate by incorporating the Michaelis-Menten constants and incorporates the nutritional value of meals remaining in the midgut at the time the current meal is consumed. The choice of (31) was made to correspond to the time it would take for the entire substrate to be consumed by reaction if the reaction rate was to proceed at maximum rate (W^m) for the entire length of the midgut. The reader is referred to Wolesensky *et al* (2004) for an equation of midgut speed that is derived to fit the empirical data presented in Yang & Joern (1994) for protein. We use a theoretical model in this paper since our goal is to only examine the qualitative response of the model under various food scenarios. Also, the nutrients referred to in the sequel are generic.

5.5 The Scaled Model

To reduce the number of parameters in the model, and thereby simplify it, we nondimensionalize. The dimensionless variables are defined by

$$\begin{aligned} v &= V/V_0,\ s_i^c = S_i^c/S_{\max},\ n_i^c = N_i^c/S_{\max},\ q_n = Q_n/(AC_{ave}), \\ s_i^m &= S_i^m/S_{\max}, n_i^m = N_i^m/S_{\max},\ c_n = C_n/C_{ave},\ y = x/L, \\ n_i^h &= N_i^h/S_{\max},\ \tau = t/(L/C_{ave}),\ T = \theta/\theta_0. \end{aligned}$$

In each case, the dimensionless variable is defined by the original dimensioned variable divided by a scale representing a characteristic value for that variable. For $S_{\max}$ we use the maximum of the two substrate concentrations that are possible in the ingested food, and C_{ave} is computed by $F(S_n)$, where S_n represents the combined average of the two substrate concentrations that are being considered. For example, if a food contains 14% protein and 7% digestible carbohydrate, then $S_n = 0.105$.

In dimensionless form, equations (18)–(23) for the substrates and nutrients in the crop become ($i = 1, 2$)

$$\frac{ds_i^c}{d\tau} = -\left(\frac{\alpha_i^c s_i^c}{\beta_i^c + s_i^c}\right) 2^{\frac{\theta_o(T-1)}{10}}, \quad s_i^c(\tau_n) = s_i^n, \quad v(\tau) \neq 0, \quad (33)$$

$$\frac{dn_i^c}{d\tau} = \left[\left(\frac{\alpha_i^c s_i^c}{\beta_i^c + s_i^c}\right) - \left(\frac{\gamma_i^c n_i^c}{\rho_i^c + n_i^c}\right)\right] 2^{\frac{\theta_o(T-1)}{10}}, \quad n_i^c(\tau_n) = 0, \quad v(\tau) \neq 0, \quad (34)$$

$$s_i^c(\tau) = 0 \text{ and } n_i^c(\tau) = 0 \text{ when } v(\tau) = 0, \quad (35)$$

$$v(\tau) = 1 - \xi^c q_n(\tau - \tau_n), \quad \tau_n \leq \tau < \tau_e, \quad (36)$$

$$v(\tau) = 0, \quad \tau_e \leq \tau < \tau_{n+1}, \quad (37)$$

where the dimensionless constants are given by

$$\alpha_i^c = \frac{LW_i^c}{C_{ave} S_{\max}},\ \beta_i^c = \frac{K_i^c}{S_{\max}},\ \gamma_i^c = \frac{LJ_i^c}{C_{ave} S_{\max}},\ \rho_i^c = \frac{M_i^c}{S_{\max}},\ \xi^c = \frac{AL}{V_0}.$$

Under the same scaling, equations (24)–(27) for the midgut are transformed into the dimensionless equations

$$\frac{\partial s_i^m}{\partial \tau} + c\frac{\partial s_i^m}{\partial y} = -\left(\frac{\alpha_i^m s_i^m}{\beta_i^m + s_i^m}\right) 2^{(\theta_o/10)(T-1)}, \tag{38}$$

$$s_i^m(y,0) = 0,\ s_i^m(0,\tau) = s_i^c(\tau), \tag{39}$$

$$\frac{\partial n_i^m}{\partial \tau} + c_n\frac{\partial n_i^m}{\partial y} = \left[\left(\frac{\alpha_i^m s_i^m}{\beta_i^m + s_i^m}\right) - \left(\frac{\gamma_i^m n_i^m}{\rho_i^m + n_i^m}\right) \times r_i\right] 2^{(\theta_o/10)(T-1)}, \tag{40}$$

$$n_i^m(y,0) = 0, \quad n_i^m(0,\tau) = n_i^c(\tau), \tag{41}$$

with dimensionless constants

$$\alpha_i^m = \frac{LW_i^m}{C_{ave}S_{\max}},\ \beta_i^m = \frac{K_i^m}{S_{\max}},\ \gamma_i^m = \frac{LJ_i^m}{C_{ave}S_{\max}},\ \rho_i^m = \frac{M_i^m}{S_{\max}}.$$

Finally, equations (30) for the nutrient concentrations in the hemolymph are given in dimensionless form as

$$\frac{dn_i^h}{dt} = \alpha_i^h \int_0^1 \left(\frac{n_i^m}{\rho_i^m + n_i^m}\right) 2^{(\theta_o/10)(T-1)} \times r_i\, dy + \gamma_i^h \left(\frac{n_i^c}{\rho_i^c + n_i^c}\right) 2^{(\theta_o/10)(T-1)} - \rho_i^h n_i^h 2^{(\theta_o/10)(T-1)} - \varepsilon_i^h, \tag{42}$$

$$n_i^h(0) = n_{i_0}^h, \tag{43}$$

with dimensionless constants given by

$$\alpha_i^h = \frac{AL\gamma_i^m}{V^h},\ \gamma_i^h = \frac{V_0\gamma_i^c}{V^h},\ \rho_i^h = \frac{\lambda_i^h L}{C_{ave}},\ \varepsilon_i^h = \frac{Ld_i}{S_{\max}C_{ave}V^h}.$$

The scaled controls for simulating post-ingestive changes are given by

$$r_1 = \begin{cases} 1, \text{ if } n_1^h(\tau_n) \le n_2^h(\tau_n), \\ \frac{n_2^h(t_n)}{n_1^h(t_n)}, \text{ if } n_1^h(\tau_n) > n_2^h(\tau_n), \end{cases} \tag{44}$$

$$r_2 = \begin{cases} 1, \text{ if } n_2^h(\tau_n) \le n_1^h(\tau_n), \\ \frac{n_1^h(t_n)}{n_2^h(t_n)}, \text{ if } n_2^h(\tau_n) > n_1^h(\tau_n), \end{cases} \tag{45}$$

while the scaled upper (u_h^i) and lower (u_l^i) thresholds for the hemolymph concentrations are

$$u_h^i = U_h^i/S_{\max},\ u_l^i = U_l^i/S_{\max}. \tag{46}$$

The scaled formula for the computation of digesta flow-through speed is given by

$$c_n = f(s_n), \tag{47}$$

where

$$f(s_n^c) = w_n\frac{\alpha^m}{\beta^m + s_n^c} \tag{48}$$

and

$$\alpha^m = \frac{LW^m}{C_{ave}S_{\max}} \text{ and } \beta^m = \frac{K^m}{S_{\max}}.$$

The scaled exponential random variable for the intermeal interval is

$$Pr(R_e \leq \tau) = 1 - \exp(-\kappa\tau), \quad \kappa = (\eta L/Q_{ave}). \tag{49}$$

In summary, equations (33)–(43) along with the feedbacks (44)–(49) give the complete scaled version of a chemical reactor model for insect digestion involving two substrates that react with enzymes to give two nutrient products. The model allows for the existence of a post-ingestive control that acts to reduce the absorption of the non-limiting nutrient across the gut wall. While the model does not lend itself to analytic techniques, it is quite tractable numerically. We use finite difference methods for the partial differential equations, a Runge–Kutta method for the ordinary differential equations, and the trapezoidal method to approximate the nonlocal term.

6 SIMULATIONS

We next use the model to determine the location of nutrient targets and simulate the behavior of an insect faced with no alternative but to ingest a single suboptimal food.

6.1 Locating the Targets

Earlier we discussed the existence of the nutrient target, growth target, intake target, and uptake target. Estimating the position of these targets is generally accomplished in one of three ways (Raubenheimer & Simpson, 1993; Simpson & Raubenheimer, 2000): (i) functionally, by adding a fitness axis to nutrient space and deriving fitness criteria by measuring performance and reproductive variability; (ii) by asking the animal to defend target points in nutrient space and then assuming that these points of homeostasis represent maximum fitness; (iii) use measurements of growth, respiration, and wastage to find the location of the targets. For a thorough discussion of identifying the location of the various targets the reader is referred to Raubenheimer & Simpson (1993). By definition,

$$NT = GT + M, \tag{50}$$

$$UT = \frac{NT}{E}, \tag{51}$$

and

$$IT = \frac{NT}{U}, \tag{52}$$

where NT, GT, IT, and UT represent the coordinates of the nutrient target, growth target, intake target, and uptake target, respectively. We use M to represent the nutrients contribution to other metabolism, E the efficiency with which nutrients are utilized from the hemolymph, and U the overall efficiency with which the nutrient is utilized once ingested. Equation (50) is a statement that the ingested nutrients must meet the demands of the animal's energy budget for growth and metabolism. Efficiency of nutrient utilization is built in the model through the kinetics for both the substrate reaction and nutrient absorption terms in the crop, midgut , and hemolymph equations. We remark that in the theoretical case of an animal having complete nutrient utilization efficiency ($U = 1,\ E = 1$), the uptake target, nutrient target and the intake target correspond to the same point in nutrient space.

The absorption terms in the hemolymph equations (30) represent the growth and metabolic contributions to an animal's energy budget. Working under the assumption that we know what ratio of nutrients constitute an optimal food, our model allows us to make *a priori* estimates for the various targets. This is of theoretical significance since an *a priori* estimate for these targets is generally not possible.

In the remainder of this section we use the model to predict the location of the uptake target and then examine the model's response to feeding on a single suboptimal food. In our model we have uptake into the hemolymph occurring in both the crop and the midgut. For the nutrients $\mathbf{N}_1$ and $\mathbf{N}_2$ we compute at time $\tau = \tau_e$,

$$\text{total uptake for } \mathbf{N}_i = \int_0^{\tau_e} \left[\int_0^1 \left(\frac{\gamma_i^m n_i^m}{\rho_i^m + n_i^m} \right) \times r_i \, dy + \left(\frac{\gamma_i^c n_i^c}{\rho_i^c + n_i^c} \right) \right] 2^{\frac{\theta_o (T-1)}{10}} \, d\tau. \tag{53}$$

We may simplify these equations by ignoring contributions from the crop. This assumption is motivated by the short residence time of food in the crop and the small values for the kinetics that occur there ($\gamma_i^c << \gamma_i^m$). Removing this uptake term, equation (53) becomes

$$\text{total uptake for } \mathbf{N}_i = \int_0^{\tau_e} \left[\int_0^1 \left(\frac{\gamma_i^m n_i^m}{\rho_i^m + n_i^m} \right) \times r_i \, dy \right] 2^{(\theta_o/10)(T-1)} \, d\tau. \tag{54}$$

If we have *a priori* knowledge of the composition of nutrients in an optimal food, we can use the model to predict the location of the uptake target at any time. This can be done by numerically solving the model using the assumption that an optimal food is being ingested for a given period of time. By computing the total uptake for the nutrients during that time we will be able to estimate the uptake target. In the sequel we present results pertaining to grasshoppers and locusts, but the model could be adjusted for other animals.

6.2 Results, Predictions, and Discussion

In this section we will often refer to the two nutrients as protein and carbohydrate because these are two of the major macro-nutrients for grasshoppers; but the discussion readily applies for other nutrients or elements. For the composition of the optimal food we use a food containing a balanced ratio of protein to nitrogen (Chambers *et al.*, 1995; Simpson & Raubenheimer, 2000) with the concentration of each being 14% dry volume. The numerical model will simulate $6\frac{1}{2}$ days. We use the following parameter values:

$A = 0.4\pi$ mm^2	$\theta_0 = 25^\circ$	$A_\theta = 10^\circ$
$W_i^m = 1$ mg/ml/hr	$W_i^c = 0.01$ mg/ml/hr	$K_i^m = 3.86$ mg/ml
$J_i^c = 0.1$ mg/ml//hr	$\lambda_i^h = 7.85$/hr	$K_i^c = 3.86$ mg/ml
$V_0 = 90$ μl	$U_h^i = 0.08$ mg/ml	$U_l^i = 0.06$ mg/ml
$L = 20$ mm	$S_{\max} = 0.23$ mg/ml	$V^h = 180$ μl
$J_i^m = 1$ mg/ml/hr	$M_i^c = 4$ mg/ml/hr	$M_i^m = 4$ mg/ml
$d_i = 0.12$ mg/hr	$Q_{ave} = 5$ mm/hr	$w_{all} = 1/k$

To predict the location of the uptake target, we simulate a no-choice assay where the insect has continuous access to a single optimal food. We let the numerical model simulate 156 hours ($6\frac{1}{2}$ days), during which we keep track of the total uptake of

both nutrients from the midgut into the hemolymph. The point in nutrient space that corresponds to these totals then serves as the uptake target. In general, the uptake target and optimal food composition are not static, but change in time. For grasshoppers the uptake target changes with respect to the length of time that is has spent in its current stadium (instar) (Simpson and Simpson, 1990). For example, the intake target and composition of an optimal food for a grasshopper will depend greatly on whether the insect is trying to gain nutrients for structure (greater need for protein) or if the goal is to meet energetic requirements (increased need for carbohydrates) (Simpson & Raubenheimer, 1993b).

We assume that the kinetics governing the substrate reactions are the same for both $\mathbf{S}_1$ and $\mathbf{S}_2$. We make a similar assumption for the kinetics governing the absorption of $\mathbf{N}_1$ and $\mathbf{N}_2$. This simplification allows for both the intake target and uptake target to be located on the same rail. We make note that for most insects dietary protein is utilized less efficiently than digestible carbohydrate (Zanotto *et al*, 1993; Waldbauer, 1968), thus we would expect the intake target and uptake target to be located at different positions in nutrient space. Currently we are interested in the comparative analysis of the model when the parameters for food quality are varied. This consists of performing a simulation under optimal food conditions and then comparing it to simulations when suboptimal values are used for the food parameters. The comparison involves examining what effect the post-ingestive control and dilution factor have on pre- and post-ingestive behavior. For this reason the choice of the parameters used in the kinetics in the model is purely speculative, and we reiterate that to accurately compare the model's response under various food qualities it is adequate that the parameters simply remain the same for each simulation.

The model makes clear predictions concerning the effect that temperature, post-ingestive control, and food quality have on eating and intermeal behavior. Figure 12 provides a comparison of the volume of material in the crop for the three different scenarios: optimal food, suboptimal food with no pre- or post-ingestive compensation, and suboptimal food with pre- and post-ingestive compensation. For a suboptimal food we assume a composition of 14% $\mathbf{S}_1$ and 7% $\mathbf{S}_2$. Figure 12a is a simulation for the response of an insect when presented with a single optimal food. The model predicts that the insect will eat approximately 7 times per day, with the insect being approximately twice as likely to eat during periods of above average temperature (Figure 12d shows the temperature cycle). This corresponds nicely to data indicating that grasshoppers are twice as likely to eating during periods of light (higher temperatures) as compared to periods of dark (low temperatures) (Simpson & Raubenheimer, 2000). Figure 12b is the model's prediction in the case of a suboptimal food with the assumption that no pre- or post-ingestive mechanism is being employed by the insect. Now the model predicts the ingestion of approximately 9 meals per day (an approximate increase of 28%). The clusters of feeding activity around periods of higher temperature again illustrates the sensitivity of the model to temperature. The enhanced feeding is a result of the model being unable to exceed the upper threshold for nutrient $\mathbf{N}_2$ (Figure 13) in the hemolymph; thus the intermeal interval is singularly determined by the random variable used to simulate a foraging delay. The effect that the pre- and post-ingestive mechanisms have on feeding behavior when the insect is presented with a single suboptimal food is shown in Figure 12c. In this case we predict the insect to ingest 12 meals per day, an increase of 70% over the optimal case. This result correlates well with data indicating that when faced with food containing a nutrient diluted to half its optimal level, grasshoppers compensate by ingesting approximately twice as much food, and

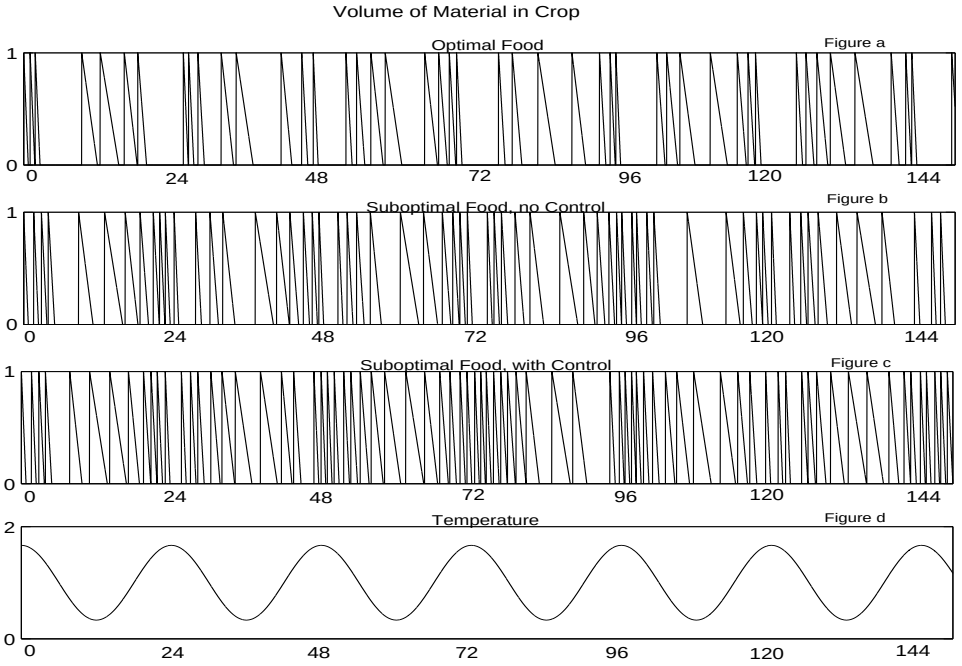

Figure 12: This figure shows the volume of material in the crop. The horizontal axis represents time in hours and the vertical axis in the top three figures is the scaled volume. Figures 12a, 12b, and 12c correspond to the three cases being considered. Note the increased consumption that is predicted for feeding on a suboptimal food. Figure 12d allows for comparison with the daily temperature cycle.

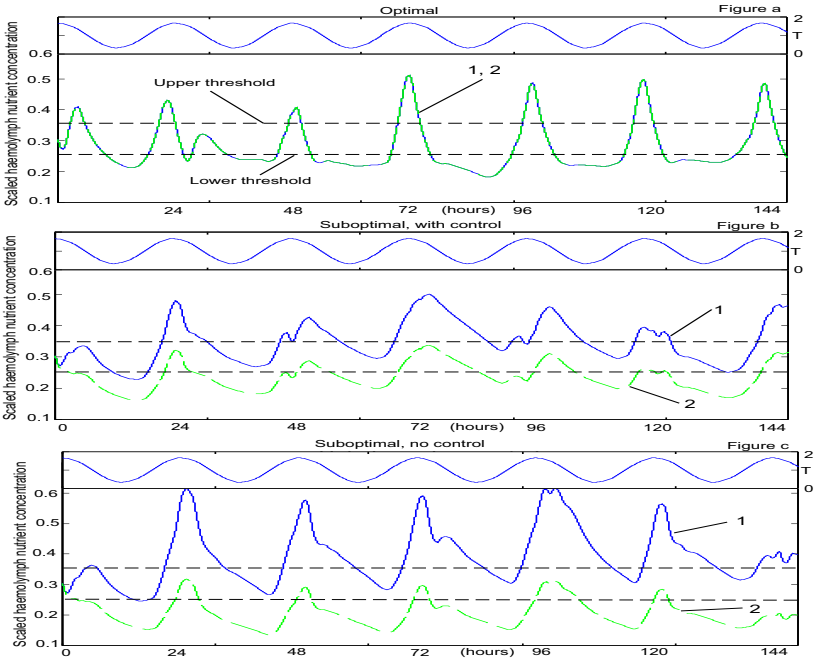

Figure 13: Graphs of nutrient levels in the hemolymph. The vertical axis represents the scaled nutrient concentrations. The optimal case is shown in figure a. In the optimal case both nutrient levels are the same since we have used identical kinetics. In figure b we see the effect of the control on nutrient levels in the suboptimal case. Figure c represents nutrient titers for a suboptimal food when no pre- or post-ingestive controls are employed.

they accomplish this by eating meals of the same size more frequently (Simpson & Simpson, 1990).

In the model we have allowed for the frequency of meals to be influenced by two factors: an exponential random variable that simulates the intermeal delay due to foraging behavior, and nutrient levels in the hemolymph. The predicted nutrient concentrations in the hemolymph are shown in Figure 13. Superimposed at the top of each plot in Figure 13 is the imposed temperature cycle. Figure 13a represents the nutrient concentrations under the assumption of an optimal food. In this case the titers for both nutrients are the same since we assumed identical kinetics and that the optimal food contains equal concentrations of the two substrates. We could easily adjust the model for other kinetics, but the main goal is to examine the qualitative changes predicted by the model for various inputs. In that regard we make note of the different predictions for the hemolymph concentrations given in Figures 13a and 13b. In Figure 13b the limiting nutrient never exceeds the upper nutrient threshold u_h^2, and thus the gustatory responsiveness of the insect is predicted to remain continually high. This leads to the compensatory behavior demonstrated in Figure 12c of increased eating. This predicted behavior has been observed in the laboratory for various insects (Simpson & Simpson, 1990; Simpson & Raubenheimer, 1993a; Chambers *et al,* 1995), and again we see congruence between the behavior predicted by the model and that of actual insect behavior. Upon comparing Figures 13b and 13c we clearly see the effect that the post-ingestive control is having on the predicted nutrient concentrations in the hemolymph.

There are two marked differences between Figure 13b (control) and Figure 13c (no control). The first is that the post-ingestive control is definitely effective in limiting the uptake of the excessive nutrient into the hemolymph. The peak levels of n_1^h for the control case (Figure 13b) are consistently between 15% to 20% lower then the peak levels for n_1^h corresponding to the no control case (Figure 13c). This difference is magnified when we take into account that, in the control case, the model predicts the ingestion rate is approximately 30% higher (due to the dilution factor) than when no control is employed (12 meals/day compared to 9 meals/day). The second major difference is in n_2^h, the concentration levels of the limited nutrient. The titer of the deficient nutrient $\mathbf{N}_2$ is approximately 30% higher in the control case than in the no control case. This is caused by the increased ingestion rate in the control case. When taken together, these differences give strong evidence that the model simulates two desired compensatory behaviors: a post ingestive compensation that limits the absorption from the midgut of the nutrient that is excessive in the hemolymph, and a pre-ingestive compensation by increasing the ingestion rate in order to elevate the titers of the limited nutrient in the hemolymph.

The model also gives considerable insight into the role of temperature in insect digestion. In Figures 13a, 13b, and 13c we see correlation between high temperatures and high nutrient concentrations in the hemolymph. This dependence on temperature is further illustrated in Figure 14 where we see the cumulative uptake of nutrient $\mathbf{N}_1$ and $\mathbf{N}_2$ into the hemolymph for each of the three cases. The cycles of rapid uptake appear to have a period of 24 hours. This corresponds to the warmest times of the daily temperature cycle, which in turn correspond to intervals of elevated hemolymph titers (Figure 13). Figure 14 also provides evidence of the reliability of the numerical model in that each result continues to be consistent with the previous results. For example, the time intervals with the highest ingestion rate (Figure 12) correspond with elevated nutrient concentrations in the hemolymph (Figure 13), which in turn correspond to the intervals of highest uptake (Figure 14). We also observe numerical consistency in the results for the three scenarios

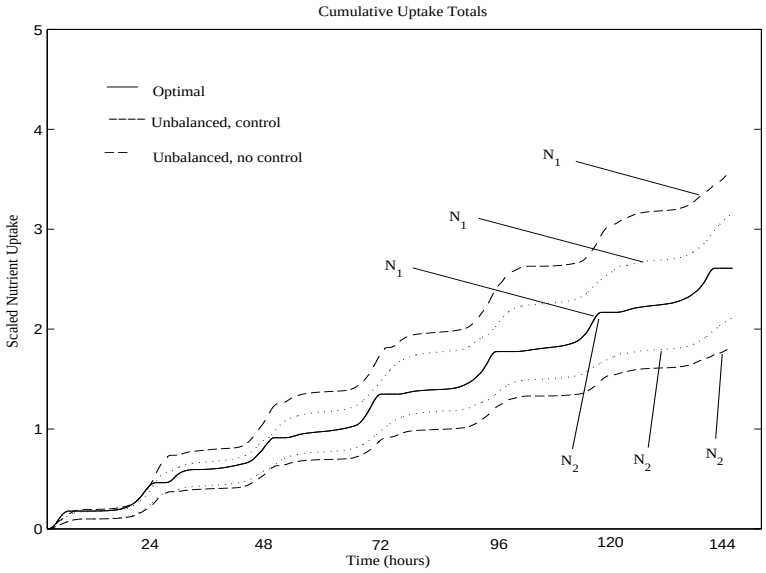

Figure 14: Cumulative uptake total for nutrient uptake in each of the three cases. The effectiveness of the controls are clearly seen when comparing the control and no control totals.

that are considered. That is, in Figure 14 we see the expected hierarchy in the cumulative uptake of the two nutrients. For $\mathbf{N}_1$ the highest uptake occurs in the case of the suboptimal food with no control, followed by suboptimal with pre- and post-ingestive controls; the lowest uptake occurs in the optimal food case, while for the limited nutrient $\mathbf{N}_2$ we see the opposite hierarchy (Figure 14).

We now use the cumulative uptake for the optimal food case to infer a prediction for the location of the uptake target (per the given parameters). The uptake target corresponds to the cumulative total for the optimal food given in Figure 14, and it lies upon the rail defined by the optimal food. Figure 15 shows the predicted location of the uptake target after $6\frac{1}{2}$ days to be (2.6, 2.6) (designated by $\mathbf{x}$). We also show in Figure 15 the rail corresponding to the suboptimal food. The point (3.5, 1.7) (designated by $\mathbf{z}$) on this rail corresponds to the predicted point in nutrient space that the animal would arrive at if it fed continually on this suboptimal food for $6\frac{1}{2}$ days and employed no pre- or post-ingestive compensatory behavior. The point (3.2, 2.1) (designated by $\mathbf{y}$) is the predicted location in nutrient space when feeding on the suboptimal food for $6\frac{1}{2}$ days, but employing the post-ingestive control and dilution factor. In all three cases the combined total uptake for the two nutrients is approximately the same. This pattern of eating behavior has been demonstrated by the desert locust, *S. gregaria* (Simpson & Raubenheimer, 2000). Animals exhibiting this form of compromise are said to use the *equi-distant rule* for feeding.

We get a better view of the uptake adjustment created by post-ingestive control in Figure 16. Here we show an exploded view near the origin of Figure 15. The point $\mathbf{C}$ represents the first adjustment made by the control and is made at the time the second meal is consumed This is equivalent to "jumping" rails through post-ingestive compensation in order to avoid "jamming" of the regulatory system. Although not as significant as the first adjustment, point D is the location of the next

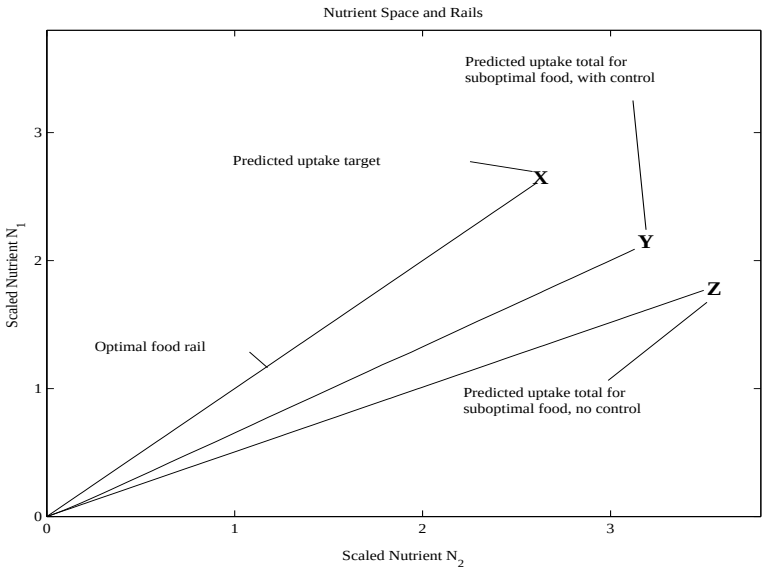

Figure 15: Uptake rails for the optimal and suboptimal food are shown. The plot of the suboptimal with controls illustrates the adjustments that the post-ingestive control and dilution factor are having on nutrient uptake. The optimal food rail represents a straight line with slope 1, while the suboptimal rail with no control is also a straight line with slope 1/2.

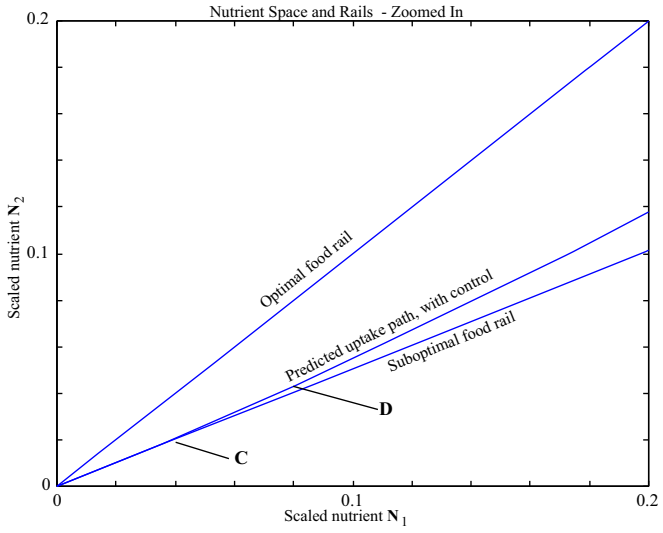

Figure 16: Exploded view of figure 15. Point C represents the adjustment of the post-ingestive control at the time the second meal is consumed. Point D shows the effect of the control when the third meal is ingested.

change in the control factor, and it occurs at the time the third meal is ingested. Subsequent adjustments of the control factor continue to occur, but on a much lessor scale; this indicates that the simulated ratio of nutrients in the hemolymph is reaching an equilibrium. Working under the assumption that the model is accurately describing the digestion process, this indicates that there could be constraints on the post-ingestive response to feeding on a suboptimal food. Although insects exhibit remarkable compensatory behavior for surviving on suboptimal foods, there is clearly a lower limit to the food quality that can be tolerated. McGinnis & Kasting (1967) showed that when the diet of fifth-instar nymphs was diluted to 1/16-th of the control diet, the compensatory ability of the nymphs were exceeded and high mortality resulted. Future work with this model includes examining the response to various ratios.

7 CONCLUSIONS

This work lays the framework for using chemical reactors to understand the link between insect foraging and digestion behavior in the context of a regulatory physiology in a multidimensional nutrient space. In comparing the results from three different scenarios the model produces results that simulated observed qualitative insect behavior. The model simulates the eating behavior of insects, in particular grasshoppers or locusts, when faced with the dilemma of meeting nutritional goals on a single suboptimal food. Laboratory experiments confirm that grasshoppers will vigorously defend certain nutrient and growth targets when faced with less than desirable foods (Simpson & Raubenheimer, 1995; Chambers *et al.*, 1998). This empirical evidence strongly suggests that insects have mechanisms that allow them to compensate both pre- and post-ingestively for deficiencies in a suboptimal food. We have modeled the pre-ingestive mechanism by a dilution factor D_f that acts to shorten the inter-meal interval, and the post-ingestive compensation by a control factor that limits uptake from the midgut of the excess nutrient.

By invoking these mechanisms the numerical model succeeded in simulating the qualitative differences in behavior that have been observed experimentally. These include increasing ingestion by approximately a factor of two when the limited nutrient is half its optimal concentration, increasing egestion of the excess nutrient by limiting its absorption, and simulating the observed uptake behavior of animals who use the equi-distance rule when feeding on suboptimal food. Agreement of the model with observed laboratory behavior supports evidence that animals possess compensatory mechanisms that allow them maintain nutritional homeostasis for a variety of food composition. The model predicts strong dependence upon temperature in the regulation of all aspects of behavior. Special note is made of the correspondence between elevated nutrient titers in the hemolymph and elevated temperature, which implies that most nutritional gain occurs during the daylight hours. Additionally, the model may be of value in making predictions regarding the effects that global temperature changes have on insect foraging and digestion.

The model also has the potential to predict *a priori* the location of the uptake target if the nutrient composition of the optimal food is known. This requires estimation of the many parameters used in the model for the various kinetics. Once the parameters are estimated, the model can be used to evaluate the efficiency of an animal's digestion system. This may be accomplished by comparing the predicted amount of nutrient ingested to the predicted amount of nutrient uptake. The success of the model in making accurate, quantitative predictions depends greatly on the

accuracy of the parameter values. Future refinements of the model include allowing for radial dependence in the composition of digesta in the midgut (as in Woods and Kingsolver, 1999), parameter estimation, and temperature comparisons.

Acknowledgements. This research was supported by the Biological and Environmental Research Program (BER), U.S. Department of Energy, through the Great Plains Regional Center of the National Institute for Global Environmental Change (NIGEC) under Cooperative Agreement No. DE-FC02-03ER63613. The authors warmly thank our colleague and oftentimes mentor, Professor Tony Joern at Kansas State University, for his overwhelming support and enthusiasm on our joint projects.

References

[1] Abisgold, J.D. & Simpson, S.J. (1987) The physiology of compensation by locusts for changes in dietary protein, *Journal of Experimental Biology* **129**, 329–346.

[2] Alberts, B. (1994) *Molecular Biology of the Cell*, 4rd ed., New York: Garland Publications.

[3] Anderson, T. R. & Hessen, D. O. (1995) Carbon or nitrogen limitation in marine copepods, *J. Plankton Research* **14**, 1645–1671.

[4] Behmer, S. T. & Joern, A. (1993) Diet choice by a grass-feeding grasshopper based on the need for a limiting nutrient, *Functional Ecology* **7**, 522–527.

[5] Behmer, S. T., Raubenheimer, D., & Simpson, S.J. (2001) Frequency-dependent food selection in locusts: a geometric analysis of the role of nutrient balancing, *Animal Behaviour* **61**, 995–1005.

[6] Belovsky, G. E. (1997) Optimal foraging and community structure: the allometry of herbivore food selection and competition, *Evol. Ecol.* **11**, 641–672.

[7] Bernays, E. A. & Bright, K. L. (1993) Mechanisms of dietary mixing in grasshoppers: a review, *Comp. Biochem. Physiol.* **104A**, 125–131.

[8] Bernays, E. A. & Simpson, S. J. (1990) Nutrition. In: *Biology of Grasshoppers* (R.F. Chapman & A. Joern, eds), pp. 105-129. New York: John Wiley and Sons.

[9] Bloom, A. J., Chapin III, F. S. & Mooney, H. A. (1985) Resource limitation in plants–an economic analogy, *Annual Review of Ecology and Systematics* **16**, 363–392.

[10] Brett, M. (1993) Comment on "Possibility of N or P limitation for planktonic cladocerans: an experimental test" (J. Urabe & J. Watanabe) and "Nutrient element limitation of zooplankton production" (D. O. Hessen), *Limnology and Oceanography* **38**, 1333–1337.

[11] Chambers, P. G., Raubenheimer, D., & Simpson, S.J. (1998) The functional significance of switching interval in food mixing by *Locusta migratoria*, *J. Insect Physiol.*, **44**, 77–85.

[12] Chambers, P. G., Raubenheimer, D., & Simpson, S. J. (1995) Behavioural mechanisms of nutrient balancing in *Locusta migratoria* nymphs, *Animal Behav.* **50**, 1513–1523.

[13] Chappel, M. A. & Whitman, D. W. (1990) Grasshopper Thermoregulation. In: *Biology of Grasshoppers* (R.F. Chapman & A. Joern, eds), pp. 143–172. New York : John Wiley and Sons.

[14] Cohen, R. W., Heydon, S. L., Waldbauer, G. P. & Friedman, S. (1987a) Nutrient self-selection by the omnivorous cockroach *Supella longipalpa*, *J. Insect Physiol.* **33**, 77–82.

[15] Cohen, R. W., Waldbauer, G. P., Friedman S. & Schiff N.M. (1987b) Nutrient self-selection by *Heliothis zea* larvae: a time-lapse film study, *Entomol. Exp. Appl.* **44**, 65-73.

[16] Dade, W. B., Jumars, P. A. & Penry, D. L. (1990) Supply-side optimization: maximizing absorptive rates. In: *Behavioral Mechanisms of Food Selection* (R. N. Hughes, ed), NATO ASI series, Volume **G 20**, pp. 531–55. Berlin: Springer-Verlag.

[17] DeAngelis, D. L. (1992) *Dynamics of Nutrient Cycling and Food Webs*, London: Chapman-Hall.

[18] Edelstein-Keshet, L. (1988) *Mathematical Models in Biology*, New York: McGraw-Hill.

[19] Frost, P. C. & Elser, J. J. (2002) Growth responses of littoral mayflies to the phosphorus content of their food, *Ecology Letters* **5,** 232–240.

[20] Gilbert, N. & Raworth, D. A. (1996) Insects and temperature–A general theory, *The Canadian Entomologist* **128**: 1–13

[21] Gross, L. J. (1986) An overview of foraging theory. In: *Biomathematics, Mathematical Ecology* Vol 17 (T.G. Hallam and S.A. Levin, eds), pp 37–57, Berlin: Springer-Verlag.

[22] Gurney, W. C. & Nisbet, R. M. (1998) *Ecological Dynamics*, Oxford: Oxford University Press.

[23] Harrison, J. F. & Fewell, J. H. (1995) Thermal effects on feeding behavior and net energy intake in a grasshopper experiencing large diurnal fluctuations in body temperature, *Physiological Zoology* **68**, 453–473.

[24] Hoffman, K. H. (1984) Metabolic and enzyme adaption to temperature. In: *Enviornmental Physiology and Biochemistry of Insects* (K.H. Hoffman, ed) pp. 1–32. Berlin: Springer-Verlag.

[25] Jumars, P. A. (2000a) Animal guts as ideal chemical reactors: Maximizing absorption rates, *Amer. Nat.* **155**(4), 527–543.

[26] Jumars, P. A. (2000b) Animal guts as nonideal chemical reactors: partial mixing and axial variation in absorption kinetics, *Amer. Nat.* **155**(4), 544–555.

[27] Jumars, P. A. & Martínez del Rio, C. (1999) The tau of continuous feeding on simple foods, *Physiol.Biochem. Zool.* **72**(5), 633–641.

[28] Karasov, W. H. (1988) Nutrient transport across vertebrate intestine. In: *Advances in Comparative and Enviornmental Physiology*, Vol. 2 (R. Gilles, ed). Berlin: Springer-Verlag.

[29] Karasov, W. H. & Hume, I. D. (1997) Vertebrate gastrointestinal system. In *Handbook of Physiology*, Section 13. Comparative Physiology. (W. H. Dantzler, ed.), Oxford: Oxford University Press.

[30] Kooijman, S. A. L. M. (1995) The stoichiometry of animal energetics, *J. Theoretical Biol.* **177**, 139–149.

[31] Kooijman, S. A. L. M. (2000) *Dynamic Energy and Mass Budgets in Biological Systems*, Cambridge: Cambridge University Press.

[32] Ledder, G. (2005) *Differential Equations: A Modeling Approach*, New York: McGraw-Hill.

[33] Lee. K. P., Behmer, S. T., Simpson, S. J., & Raubenheimer, D. (2002) A geometric analysis of nutrient regulation in the generalist caterpillar *Spodoptera littoralis* (Boisduval), *Journal of Insect Physiology* **48**, 655-665.

[34] Lika, K. & Nisbet, R. M. (2000) A dynamic energy budget model based on partitioning of net production, *J. Math. Biol.* **41**, 361–386.

[35] Logan, J. D., Joern, A. & Wolesensky, W. (2002) Location, time, and temperature dependence of digestion in simple animal tracts, *J. Theor. Biol.* **216**, 5–18.

[36] Logan, J. D., Joern, A. & Wolesensky, W. (2003) Chemical reactor models of optimal digestion efficiency with constant foraging costs, *Ecological Modelling* **168**, 25–38.

[37] Logan, J. D., Joern, A. & Wolesensky, W. (2004a) Control of CNP homeostasis in herbivore consumers through differential assimilation, *Bulletin of Mathematical Biology* **66**, 707–725.

[38] Logan, J. D., Joern, A. & Wolesensky, W. (2004b) Mathematical model of consumer homeostasis control in plant-herbivore dynamics, *Mathematical and Computer Modelling* (in press).

[39] Loladze, I., Kuang, Y. & Elser, J. J. (2000) Stoichiometry in producer-grazer systems: linking energy flow with element cycling, *Bull. Math. Biology* **62**, 1137–1162.

[40] Loladze, I., Kuang, Y., Elser, J. J. & Fagan, W. F. (2004). Competition and stoichiometry: coexistence of two predators on one prey, *Theor. Population Biology* **65**, 1–15.

[41] Lotka, A. (1925) *Elements of Physical Biology*, Baltimore: Williams & Wilkins.

[42] Martínez del Rio, C, Cork, S. J. & Karasov, W. H. (1994) Modelling gut function: an introduction. In *The Digestive System in Mammals*, (D. J. Chivers & P. Langer, eds), Cambridge: Cambridge University Press.

[43] Martínez del Rio, C. & Karasov, W. H. (1990) Digestion strategies in nectar and fruit-eating birds and the sugar composition of plant rewards, *Amer. Nat.* **135**, 618–637.

[44] McGinnis, A. J. and Kasting, R. (1967) Dietary cellulose; effect on food consumption and growth of a grasshopper, *Can. J. Zool.* **45**, 365.

[45] Mueller, E. B., Nisbet, R. M., Kooijman, S. A. L. M., Elser, J. J., & McCauley, E. (2001) Stoichiometric food quality and herbivore dynamics, *Ecology Letters* **4**, 519–529.

[46] Murray, J. D. (2002) *Mathematical Biology*, Vol 1, New York: Springer-Verlag.

[47] Nauman. E. B. (1987) *Chemical Reactor Design*, New York: John Wiley and Sons.

[48] Penry, D. L & Jumars, P. A. (1986) Chemical reactor analysis and optimal digestion, *Bioscience* **36**, 310–315.

[49] Penry, D. L & Jumars, P. A. (1987) Modeling animal guts as chemical reactors, *American Nat.* **129**, 69–96.

[50] Raubenheimer, D. (1992) Tannic acid, protein and digestible carbohydrate: Dietary imbalance and nutritional compensation in the African migratory locust, *Ecology* **73**, 1012–1027.

[51] Raubenheimer, D. R. & Simpson, S. J. (1993) The geometry of compensatory feeding in the locust, *Animal Behavior* **45**, 953–964.

[52] Sibly, R. M. (1980) Strategies of digestion and defecation. In: *physiological Ecology: An Evolutionary Approach to Resource Use* (C. R. Townsend and P. Calow, eds), Sunderland: Sinauer Associates, 109–139.

[53] Simpson, S. J. & Raubenheimer, D. (1993a) The central role of the haemolymph in the regulation of nutrient intake in insects, *Physiological Entomology* **18**, 395–403.

[54] Simpson, S. J. & Raubenheimer, D. (1993b) A multi-level analysis of feeding behavior: The geometry of nutritional decisions, *Philos. Trans. R. Soc. London B* **342**, 381–402.

[55] Simpson, S. J. & Raubenheimer, D. (1995) The geometric analysis of feeding and nutrition: A user's guide, *J. Insect Physiol.* **41**, 545-553.

[56] Simpson, S. J.& Raubenheimer, D. (1996) Feeding behaviour, sensory physiology and nutrient feedback: A unifying model, *Entomol. Exp. Appl.* **80**, 55–64.

[57] Simpson, S. J. & Raubenheimer, D. (2000) The hungry locust, *Adv.Study Behavior* **29**, 1–44.

[58] Simpson, S. J., Raubenheimer, D., Behmer, S. T., Whitworth, A. & Wright, G.A. (2002) A comparison of nutritional regulation in solitarious- and gregarious-phase nymphs of the desert locust *Schistocerca gregaria*, *The Journal of Experimental Biology* **205**, 121–129.

[59] Simpson S.J., Raubenheimer, D. & Chambers, P.G. (1995) Nutritional homeostasis. In: *Regulatory Mechanisms of Insect Feeding*, (R. F. Chapman and G. de Boer, eds). New York: Chapman and Hall.

[60] Simpson, S. J. & Simpson, C. L. (1990) The mechanisms of nutritional compensation by phytophagous insects. In: *Insect-plant interactions* 2 (E.A. Bernays, ed), pp. 111–160. Boca Raton: CRC Press.

[61] Srivastava, P. D. (1973) The digestive system and digestion in insects. In: *Insect Physiology and Anatomy* (N.C, Pant and S. Ghai, eds), pp. 44–54. New Delhi: Indian Council of Agricultural Research.

[62] Stephens, D. & Krebs, J. R. (1986) *Foraging Theory*, Princeton: Princeton University Press.

[63] Sterner, R. W. (1997) Modelling interactions of food quality and quantity in homeostatic consumers, *Freshwater Biology* **38**, 473–481.

[64] Sterner, R. W. & Elser, J.J. (2002) *Ecological Stoichiometry*, Princeton: Princeton University Press.

[65] Tang, K. W. & Dam, H. G. (1999) Limitation in zooplankton production: beyond stoichiometry, *Oikos* **84**, 537–542.

[66] Thingstad, T. F. (1987) Utilization of N, P, and organic C by heterotrophic bacteria, *Mar. Ecol. Prog. Ser.* **35**, 99–109.

[67] Waldbauer, G. P. (1968) The consumption and utilization of food by insects, *Adv. Insect Physiol.* **5**, 229.

[68] Waldbauer, G. P. and Friedman, S. (1991) Self-selection of optimal diets by insects. *A. Rev. Entomal.* **36**, 43–63.

[69] Whelan, C. J. & Schmidt, K. A. (2003) Food acquisition, processing and digestion, In: *Foraging*, (D. W. Stephens, J. S. Brown & R. Ydenberg, eds.), Chapter 6, Chicago: University of Chicago Press.

[70] White, T. C. R. (1993) *The Inadequate Environment: Nitrogen and the Abundance of Animals*, Berlin: Springer-Verlag.

[71] Wigglesworth, V. B. (1984) *Insect Physiology*, 8th ed. New York: Chapman and Hall.

[72] Wolesensky, W. (2002) *Mathematical Models of Digestion Modulation*, PhD dissertation, Lincoln: University of Nebraska–Lincoln.

[73] Wolesensky, W., Joern, A. & Logan, J. D. (2004) A model of digestion modulation in grasshoppers, *Ecological Modelling* In review.

[74] Woods, H. A. & Kingsolver, J. G. (1999) Feeding rate and the structure of protein digestion and absorption in Lepidopteran midguts. *Arch. Insect Biochem. and Physiology* **42**: 74–87.

[75] Wright, S. H. & Ahearn, G. A. (1997) Nutrient absorption in invertebrates, In: *Handbook of Physiology*, Vol II (W. H. Dantzler, ed), Oxford: Oxford University Press.

[76] Yang, Y. & Joern, A. (1994) Influence of diet quality, developmental stage, and temperature on food residence time in the grasshopper *Melanoplus differentialis*, *Physiological Zoology* **67**, 598–616.

[77] Zanotto, F. P., Simpson, S. J., & Raubenheimer, D. (1993) The regulation of growth by locusts through post-ingestive compensation for variation in the levels of dietary protein and carbohydrate, *Physiol Entomol.* **18**, 425–434.